



Contents lists available at ScienceDirect

Journal of Controlled Release

journal homepage: www.elsevier.com/locate/jconrel

Review

Factors controlling the pharmacokinetics, biodistribution and intratumoral penetration of nanoparticles

Q1 Mark J. Ernsting^{a,b}, Mami Murakami^a, Aniruddha Roy^a, Shyh-Dar Li^{a,c,d,*}^a Drug Delivery and Formulation, Drug Discovery Program, Ontario Institute for Cancer Research, 101 College Street, Suite 800, Toronto, Ontario M5G 0A3, Canada^b Ryerson University, Toronto, Ontario M5B 1Z2, Canada^c Leslie Dan Faculty of Pharmacy, University of Toronto, Toronto, Ontario M5S 3M2, Canada^d The Techna Institute, University Health Network, Toronto, Ontario M5G 1P5, Canada

ARTICLE INFO

Article history:

Received 7 August 2013

Accepted 15 September 2013

Available online xxx

Keywords:

Nanoparticle

Pharmacokinetics

Biodistribution

Tumor microenvironment

Intratumoral penetration

ABSTRACT

Nanoparticle drug delivery to the tumor is impacted by multiple factors: nanoparticles must evade clearance by renal filtration and the reticuloendothelial system, extravasate through the enlarged endothelial gaps in tumors, penetrate through dense stroma in the tumor microenvironment to reach the tumor cells, remain in the tumor tissue for a prolonged period of time, and finally release the active agent to induce pharmacological effect. The physicochemical properties of nanoparticles such as size, shape, surface charge, surface chemistry (PEGylation, ligand conjugation) and composition affect the pharmacokinetics, biodistribution, intratumoral penetration and tumor bioavailability. On the other hand, tumor biology (blood flow, perfusion, permeability, interstitial fluid pressure and stroma content) and patient characteristics (age, gender, tumor type, tumor location, body composition and prior treatments) also have impact on drug delivery by nanoparticles. It is now believed that both nanoparticles and the tumor microenvironment have to be optimized or adjusted for optimal delivery. This review provides a comprehensive summary of how these nanoparticle and biological factors impact nanoparticle delivery to tumors, with discussion on how the tumor microenvironment can be adjusted and how patients can be stratified by imaging methods to receive the maximal benefit of nanomedicine. Perspectives and future directions are also provided.

© 2013 Published by Elsevier B.V.

Contents

1. Introduction	0
2. Blood circulation and RES interaction	0
2.1. Strategies to reduce RES interactions	0
2.1.1. Surface decoration	0
2.1.2. Size and morphology	0
2.1.3. Composition	0
2.1.4. Zeta potential	0
2.2. RES activity and personalized dose adjustment	0
3. Nanoparticle extravasation and retention in tumors	0
3.1. Tumor vascular permeability and nanoparticle extravasation	0
3.2. Strategies to enhance the tumor extravasation of nanoparticles	0
3.2.1. Reduce particle size	0
3.2.2. Tumor blood vessel modulating treatments	0
3.3. Factors affecting tumor retention of nanoparticles	0
4. Tumor penetration of nanoparticles and drug release	0
4.1. Tumor physiological factors that impact nanoparticle penetration	0
4.1.1. Abnormal and heterogeneous vasculature	0
4.1.2. Interstitial fluid pressure (IFP)	0
4.1.3. Stromal density	0
4.1.4. Tumor associated macrophage (TAM)	0

* Corresponding author at: 101 College St, MaRS Centre South Tower, Suite 800, Toronto, Ontario M5G 0A3, Canada. Tel.: +1 647 260 7994.

E-mail address: sli@oicr.on.ca (S.-D. Li).

64	4.2.	Nanoparticle properties that impact the tumor penetration	0
65	4.2.1.	Size	0
66	4.2.2.	Zeta potential	0
67	4.2.3.	Targeting ligands	0
68	4.3.	Approaches to modulate tumor penetration of therapeutic agents	0
69	4.3.1.	IFP reduction	0
70	4.3.2.	Stromal depletion	0
71	4.4.	Drug release from nanoparticles	0
72	4.5.	Factors impacting cellular internalization of nanoparticles and the drug release	0
73	4.5.1.	Mechanisms of cellular internalization of nanoparticles	0
74	4.5.2.	Size	0
75	4.5.3.	Shape	0
76	4.5.4.	PEGylation	0
77	4.5.5.	Zeta potential	0
78	4.5.6.	Targeting ligands	0
79	4.5.7.	TAM content and drug release	0
80	5.	Conclusion and perspectives	0
81		Acknowledgment	0
82		References	0

83

84 1. Introduction

85 Nanomedicine therapies are broadly defined as active pharmaceutical
86 ingredients formulated in delivery vehicles exhibiting an average
87 size between 10 and 200 nm, and these encompass liposomes, micelles,
88 polymeric nanoparticles, dendrimers, and macromolecules. Properly for-
89 mulated nanoparticles evade the 5 nm renal filtration cutoff [1–3] and
90 exhibit prolonged blood circulation, giving these particles an increased
91 opportunity to interact with tumor tissues. Unlike normal blood vessels
92 which feature a tightly sealed endothelium, tumor vasculature tends to
93 be abnormally permeable to macromolecules and nanoparticles, and fur-
94 thermore, lymphatic drainage is generally impaired in tumors: as a result
95 of these pathological features, nanoparticles selectively accumulate in
96 this biological cul-de-sac. On the other hand, low molecular weight
97 drugs can non-selectively diffuse through the endothelial layer of normal
98 tissues, inducing significant off-target toxicity at therapeutic doses. The
99 enhanced permeability and retention (EPR) effect is the central hypoth-
100 esis and science of nanomedicine, and tumors that present with high
101 permeability are good candidates for this class of therapy.

102 Nanoparticles display distinctive pharmacokinetics (PK) and
103 biodistribution (BD) compared to small molecules, and the altered
104 *in vivo* biofate in turn alters the toxicity and efficacy profile of each
105 drug. There are three major phases in nanoparticle drug delivery
106 (Fig. 1): (1) systemic circulation and reticuloendothelial system
107 (RES) interaction, (2) extravasation and tumor penetration, and
108 lastly, (3) interaction with the target cells. This review focuses on
109 the effect of nanoparticle composition and physicochemical proper-
110 ties on the interactions with the biological systems in these three
111 phases, and how those interactions affect nanoparticle biofate.

112 2. Blood circulation and RES interaction

113 The first phase of delivery involves the systemic circulation and in-
114 teraction with the RES, a global system of macrophages in the liver,
115 spleen, and bone marrow, but with respect to nanoparticle clearance,
116 the liver and spleen are the most active. Macrophages are phagocytic
117 cells, and will engulf particles bearing recognized opsonins (serum
118 proteins) that have adsorbed to nanoparticles [4–6]. For example,
119 Nagayama et al. [7] demonstrated that the increased amount of comple-
120 ment protein C3 and immunoglobulin G (IgG) adsorbed onto the 50-nm
121 polystyrene nanoparticles in the serum was directly reflected in the in-
122 creased rate of uptake of the nanoparticles by Kupffer cells. Factors af-
123 fecting opsonization and the RES interaction include PEGylation, size,
124 composition, zeta potential, and shape of nanoparticles. Interaction of

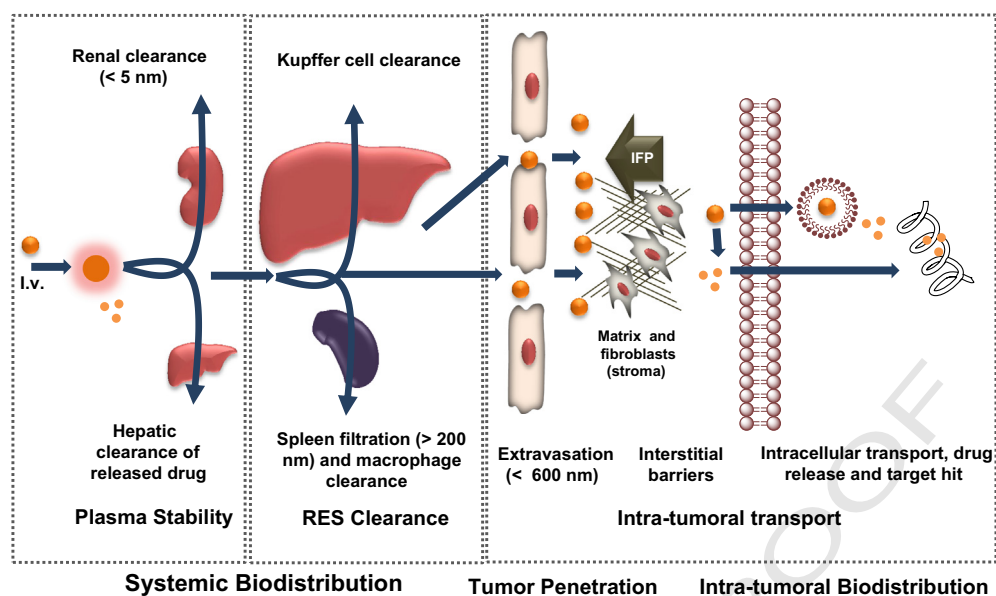
nanoparticles with the RES is a significant determinant of blood circula- 125
tion time and rates of clearance. Nanoparticles with a decreased blood 126
circulation time usually display reduced tumor uptake and efficacy. 127

2.1. Strategies to reduce RES interactions 128

2.1.1. Surface decoration 129

The most widely used surface decoration technique is introduction of 130
polyethylene glycol (PEG), which is a hydrophilic polymer, to the surface 131
of nanoparticles to reduce serum protein binding through a process of 132
steric hindrance. PEG has been deployed in various types of nanoparticles, 133
including liposomes, polymeric nanoparticles, and hybrid nanoparticles 134
[8]. Sadzuko et al. [9] reported that PEGylation led to a 3-fold reduction 135
in RES uptake, a 6-fold higher plasma area under the curve (AUC), and a 136
3-fold increased tumor uptake of a liposomal drug, leading to enhanced 137
antitumor efficacy. Similar results have been reported by others with dif- 138
ferent types of nanoparticles [10–12]. PEG creates a border around 139
nanoparticles and provides a nonspecific steric hindrance barrier 140
preventing access of proteins [13,14]. The molecular weight (MW) of 141
PEG and the amount used has an influence on performance. Fang et al. 142
[15] studied protein adsorption on 100–200 nm PEGylated nanoparticles 143
containing a range of PEG MW (2, 5, and 10 kDa), and determined that 144
10 kDa PEG was the most effective. Ernsting et al. [16] prepared 145
PEGylated cellulose drug conjugates which exhibited self-assembly prop- 146
erties dependent on hydrophobic/hydrophilic balance, and for this system 147
a 2 kDa PEG was optimal. Walkey et al. [17] utilized label-free liquid chro- 148
matography tandem mass spectrometry to determine serum protein 149
binding to gold nanoparticles possessing different surface PEG densities. 150
They reported that gold nanoparticles with different PEG densities attract 151
different clusters of serum proteins, and the cluster of proteins binding to 152
low PEG density particles (<0.16 PEG/nm²) facilitated macrophage up- 153
take. On the other hand, the cluster of proteins that bound to high PEG 154
density particles (>0.64 PEG/nm²) did not trigger serum-dependent 155
phagocytosis, and the uptake by macrophage was less efficient (Fig. 2). 156
While PEG reduces RES interactions, PEG also has an impact on particle 157
properties including stability and drug release, and for each composition 158
the MW and wt.% of PEG have to be experimentally optimized. This is a 159
well-known consideration in liposomal formulation: DSPE-PEG₂₀₀₀ is a 160
common component of PEGylated liposomes, but it has detergent proper- 161
ties, and will destabilize liposomes when exceeding 8 mol% [18]. 162

Despite the benefits that PEG confers, PEGylation is suspected to 163
induce immune responses and hypersensitivity, especially when an 164
immunostimulatory agent is included such as siRNA and pDNA 165
[19–21]. Ishida et al. [22] and Judge et al. [23] demonstrated that the 166



Q8 Fig. 1. The three phases of drug delivery by nanoparticles. Nanoparticles injected intravenously must evade RES and renal clearance, and remain stable in plasma during systemic circulation, such that a sufficient dose of nanoparticle and drug can interact with tumor physiology. Once particles successfully extravasate into the tumor compartment, the particles must travel through the stroma against high interstitial fluid pressure (IFP) gradients, and ultimately interact with the target cells or release the drug payload for pharmacological effect.

167 blood clearance of the second dose of PEGylated liposomes was accelerat- 182
 168 ed by spleen-dependent generation of specific anti-PEG IgM. Exploration 183
 169 of alternative compositions to PEG is a relatively small field. Polyamino 184
 170 acids (such as polyglutamic acid), glycopolymers, and polyoxazolines 185
 171 (POx) have been shown to assist molecules and nanoparticles to evade 186
 172 RES clearance [24,25].

173 Regardless of the mechanism by which PEG works and how well it 187
 174 improves PK and BD, significant RES clearance is still an issue, with typi- 188
 175 cally >50% of the injected dose (ID) ending up in the liver and spleen 189
 176 after 48 h even for highly optimized PEGylated particles [13,14,26,27].

177 Rodriguez and colleagues [28] conjugated a “Self” peptide on to the 190
 178 surface of a nanoparticle, and demonstrated that the macrophage- 191
 179 mediated clearance of the nanoparticles was reduced, leading to >10- 192
 180 fold prolonged blood circulation and ~4-fold increased tumor uptake 193
 181 compared to the standard PEGylated nanoparticles. The “Self” peptide 194
 195

182 was computationally designed to mimic the function of human CD47, 183
 184 which is a marker of self, impeding phagocytosis of self by signaling 185
 186 through the phagocyte receptor CD172a. 187

2.1.2. Size and morphology

185 For a nanoparticle to exhibit prolonged circulation and leverage the 186
 187 EPR effect, the lower limit of particle size is 5.5 nm, the renal filtration 188
 189 cutoff size [29]. A second lower limit is imposed by liver filtration, as vas- 190
 191 cular fenestrations in the liver are 50–100 nm, and particles smaller than 192
 193 50 nm will interact with hepatocytes. The upper limit of particle size is 194
 195 influenced by two factors: tumor permeability and splenic filtration. Vas- 196
 197 cular fenestrations vary from 400 to 600 nm to microns [30] among tu- 198
 199 mors. Liu et al. [4] investigated the BD of liposomes ranging from 30 to 200
 200 nm: 4 h after injection, liposomes ranging from 100 to 200 nm were 4-fold more concentrated in tumors compared to liposomes

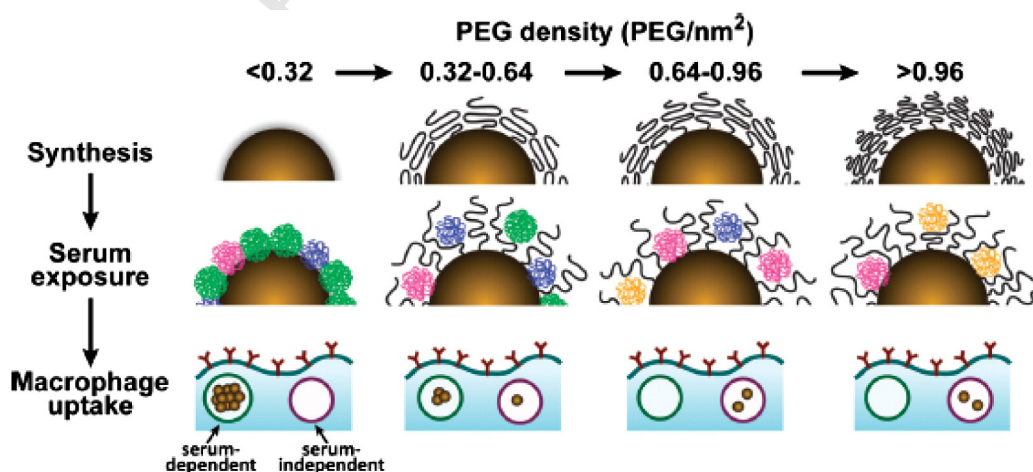


Fig. 2. Schematic illustrating the influence of PEG density on serum protein adsorption to gold nanoparticles and their subsequent uptake by macrophages. The top panel shows as-synthesized gold nanoparticles grafted with PEG at increasing density. As PEG density increases, PEG volume decreases as a result of PEG–PEG steric interactions. The middle panel illustrates how PEG density determines the amount and relative abundance of serum proteins adsorbed to the gold nanoparticle surface after serum exposure. At low PEG densities (<math>< 0.32\text{ PEG/nm}^2</math>), proteins from cluster C (green) adsorb preferentially. At low-intermediate densities ($0.32\text{--}0.64\text{ PEG/nm}^2$), proteins from cluster B (blue) adsorb preferentially. At intermediate-high PEG densities ($0.64\text{--}0.96\text{ PEG/nm}^2$), proteins from cluster C (fuchsia) adsorb preferentially. At high PEG densities (>

below 50 and above 300 nm. The liver uptake of particles below 50 and above 300 nm was 25% ID, compared to 10% ID for 100 nm liposomes. Further, particles greater than 400 nm in size were cleared in the spleen (40–50% ID). Blood components passing through the splenic sinus must pass through intercellular slits that rarely exceed 500 nm in width [31] and although the size cutoff for each nanoparticle will depend on deformability and shape, particles exceeding 300–400 nm tend to be trapped [32]. Hrkach et al. [33] generated a comprehensive series of PEG-polyester nanoparticles, examining 63 compositions ranging from 28 to 224 nm, ultimately selecting their lead formulation which was 100 nm in size. Generally, particles near 100 nm in diameter tend to represent an optimal range for leveraging the EPR effect and minimizing clearance [3]. Within a specific class of composition, size will impact protein adsorption and the resulting RES clearance. Fang et al. [15] reported that the protein adsorption on the 80-nm particles (6%) was lower than that on larger sizes (171 and 243 nm, 23 and 34%, respectively), because smaller particles exhibit a higher surface density of PEG. As a result, blood clearance of the 80 nm particles was twice as slow as with the larger nanoparticles (171 and 243 nm). Moreover, the accumulation of the 80 nm particles in the tumor within 24 h was 2-fold that of the larger nanoparticle formulations.

Particle shape is also a crucial parameter that can impact circulation time and tumor accumulation. Champion and Mitragotri [34] measured the interaction of diversely shaped micro-sized polystyrene particles with macrophages. They defined a dimensionless shape-dependent parameter related to the length normalized curvature, Ω (Fig. 3). Particles were found to be internalized successfully when $\Omega \leq 45^\circ$ (ellipsoid or sphere) via actin-cup and ring formation, with phagocytosis velocity being inversely correlated to Ω (up to 45°); on the other hand, when $\Omega > 45^\circ$ (ellipsoid), cell spreading but not internalization occurs (Fig. 3). In contrast, the contribution of particle size or volume to the phagocytotic process was evidently lower compared to particle shape, affecting the completion of particle internalization only when the particle volume is greater than that of the macrophage at Ω of $\leq 45^\circ$. They also demonstrated that a form of worm-like polystyrene particles was phagocytosed to a lesser extent by alveolar rat macrophages compared to spherical particles of equal volume. The success of the high aspect ratio particles in avoiding phagocytosis was attributed to the predominance of low curvature regions on the flat sides ($\Omega = 87.5^\circ$) over the high curvature regions ($\Omega = 2.5^\circ$), which were only present at the two discrete ends of the worm-like particles [35].

Altering particle shape away from the spherical has been shown to enhance circulation time and influence particle disposition, as these

particles exhibit altered hydrodynamic behavior that influences circulation, transport in the blood flow, and finally BD. Discher and coworkers [36] prepared filamentous micelles (filomicelles) under simulated splenic flow conditions, in which long filomicelles were formed by a solvent evaporation self-assembly process using diblock copolymers of PEG and the inert poly(ethylene) or biodegradable poly(ϵ -caprolactone): the filomicelles exhibited reduced uptake by macrophages, and exhibited persistent circulation for up to a week, which was in strong contrast with the spherical PEGylated stealth vesicles that were cleared within 2 days. The unique hydrodynamic properties of filamentous, flexible micelles allowed them to align with the blood flow, resulting in a substantial extension of the circulation time [36]. In another example, the circulation time of liposomes in the size range of 100–150 nm was enhanced by 3.6-fold via the transformation of the spherical vesicles into a disk-like vesicle [37].

2.1.3. Composition

Material hydrophobicity is commonly associated with the binding of plasma proteins [38,39]. Semple et al. [40,41] demonstrated that liposomes composed of neutral saturated lipids with carbon chains greater than C16 bound to larger quantities of blood proteins compared with their C14 counterparts. Moghimi et al. [42] demonstrated that the liposomes rich in cholesterol bound less protein than cholesterol-free liposomes due to increased rigidity in the lipid bilayer. Lipids present in the liposomes also affect the pharmacokinetic parameters. It has been shown that circulation half-life of liposomes typically increases as a function of increasing lipid dose [43,44]. This effect is likely due to a decreased phagocytic capacity of RES macrophages after the ingestion of high lipid doses or to saturation of opsonization of the circulating liposomes [45].

2.1.4. Zeta potential

The net charge on a surface of a particle is measured as zeta potential (ξ), and is an influential physical factor impacting PK and BD. Generally speaking, negative particles ($\xi \leq 10$ mV) exhibit strong RES uptake, and positive particles ($\xi > 10$ mV) will induce serum protein aggregation: neutral nanoparticles (within ± 10 mV) exhibit the least RES interaction and the longest circulation [3]. Semple et al. [40,41] showed that cationic liposomes bind 500–900 serum protein/mol lipid compared to 100 serum protein/mol lipid bound by their neutral counterparts. Xiao et al. [46] demonstrated that nanoparticles with high positive (> 10 mV) or negative surface charge (≤ 10 mV) were efficiently opsonized and cleared by the Kupffer cells from the blood circulation.

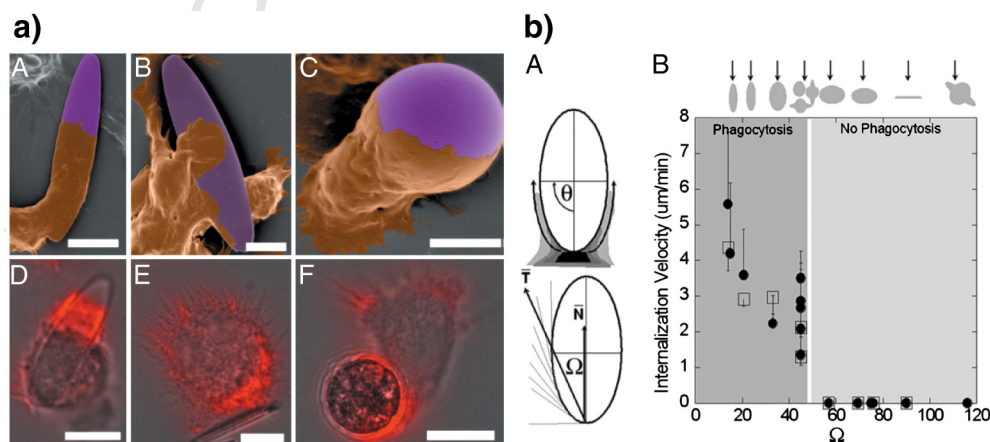


Fig. 3. Effect of target geometry in phagocytosis. (a) Scanning electron micrographs (A–C) of cells and particles were colored brown and purple, respectively. D–F are overlays of bright field and fluorescent images after fixing the cells and staining for polymerized actin with rhodamine phalloidin. A and C: The membrane has progressed down the length of the particle. B: The macrophage has spread over the flat side of an elliptical disk. D and F: Actin ring and cup, respectively, were formed as internalization begins after attachment. E: Actin polymerization occurred in the cell at site of attachment to flat side of an opsonized elliptical disk, but no actin ring or cup was visible. (b) Definition of Ω and its relation with membrane velocity. \bar{T} represents the average of tangential angles near the point of cell contact. Ω is the angle between \bar{T} and the membrane normal at the site of attachment. Adapted from ref [34]. Copyright (2006) National Academy of Science, USA. (For interpretation of the references to color in this figure legend, the reader is referred to the web version of this article.)

Levchenko et al. [47] reported similar results: particles exhibiting $\xi \leq 40$ mV exhibited >90% clearance in 10 min compared to <10% clearance for the neutral particles ($\xi \pm 10$ mV), and increased liver uptake (60% ID versus <20%ID in 1 h) was implicated in the accelerated clearance. Gessner et al. [48,49] observed an increase in plasma protein adsorption with increasing surface charge density for negatively charged polymeric nanoparticles. They also demonstrated that positively charged polystyrene nanoparticles predominantly adsorb proteins with an isoelectric point (pI) <5.5, such as albumin, while negatively charged particles adsorb proteins with a pI > 5.5, such as IgG [48,49]. Zhang et al. [50] reported that lipoplex (a positively charged complex) formed aggregates in serum, leading to transient embolism in the lungs, with ultimate clearance to the liver. In the Levchenko and Zhang studies, PEGylation served to shield the charge effect [47,50], suggesting that PEG may minimize opsonization not only through steric hindrance but also charge shielding.

2.2. RES activity and personalized dose adjustment

Nanoparticles are cleared largely by the RES [3,51,52]. Therefore, reduced RES activity will result in prolonged blood circulation of nanoparticles, which will have an increased chance to interact with other normal tissues, inducing side effects. La-Beck et al. [53] demonstrated that patients with increased RES activity (increased pre-cycle monocyte count) exhibited enhanced clearance for Doxil, which is a PEGylated liposomal doxorubicin. Therefore, an individual with reduced RES activity will display decreased clearance and increased toxicity, whereas a patient exhibiting high RES activity will experience increased clearance and reduced efficacy at the same dose. These results suggest that: first, individual dose adjustment according to the RES activity (possibly *via* pre-cycle monocyte count) is needed to optimize the treatment and minimize the side effects of nanomedicines. Second, multiple dosing should be planned carefully as the interaction between nanoparticles and the RES is bidirectional [54]: the first dose of nanoparticles may suppress the RES activity, reducing the clearance and increasing the toxicity of the subsequent doses. For example, the blood clearance of Doxil in human patients was shown to be reduced by 43% at the third dose compared to the first dose, and the skin toxicity of Doxil appeared after the third cycle [55].

3. Nanoparticle extravasation and retention in tumors

The second phase of delivery is nanoparticle extravasation from the bloodstream and retention in the tumor tissue. This process is selective for highly permeable tumors that lack lymphatic drainage.

3.1. Tumor vascular permeability and nanoparticle extravasation

Tumor blood vessels are dense, immature, chaotically branched, and dilated [56], and early in cancer research it was observed that large molecules such as proteins were leaking out of tumors, suggesting hyperpermeability [57–59]. It was further observed that blood-borne macromolecules >40 kDa and nanoparticles could evade renal clearance and leak into tumors [60]. In normal tissues (excepting the RES), the contact layer between blood and tissues is continuous and well sealed against macromolecules and particles [14], preventing extravasation of nanoparticles into most normal tissues with reduced off-target toxicity [1]. This selective extravasation effect favors long-circulating nanoparticles, as this passive targeting effect is an accumulative process. This phenomenon has been observed in both animal and human tumor biology. The earliest example was generated by the Maeda group [2,61–63]: a styrene maleic anhydride polymer was conjugated to neocarzinostatin (SMANCS), and patients treated with this therapeutic were imaged by CT, with tumor accumulation of the therapy reading 10–200 times higher than normal tissues. Harrington et al. [64]

demonstrated that ^{111}In -labeled PEGylated liposomes selectively accumulated in the liver, spleen, squamous cell tumor, cardiac blood pool, and bowel using radiographic whole body measurements, confirming the typical BD profile for long-circulating liposomes. Similar radiographic measurements in patients suffering from Kaposi's sarcoma confirmed the selective BD of Doxil [64].

Despite the dramatically improved PK, BD, efficacy and safety profiles of nanomedicines in preclinical models, most of them do not increase overall survival of patients compared to the standard chemotherapy [65]. Patients with HIV-related Kaposi's sarcoma or metastatic breast cancer receiving doxorubicin or Doxil have similar overall survival [66,67]. Similar results were shown for DaunoXome in treating patients with HIV-related Kaposi's sarcoma [68]. Although a couple of positive trials with nanomedicines have been reported, including Doxil for metastatic ovarian cancer [69] and Abraxane for metastatic breast cancer [70], the benefit of nanomedicine in clinical patients has not been consistent. Opaxio exhibited promising efficacy in preclinical models and in a small number of cancer patients in early clinical trials, but failed in phase III trials when the product was tested in a large number of patients [71]. These clinical results suggest that patients have significant variations in tumor pathophysiology, which contributes to the variable therapeutic outcomes, resulting in statistically non-significant results that mask the benefit of nanomedicine. Particularly, heterogeneous tumor vasculature is anticipated to lead to highly variable delivery of nanoparticles [65,72]. Ernstring et al. [73] recently reported that the tumor uptake and efficacy of their nanoparticles were linearly correlated with the tumor blood vessel density ($R^2 > 0.9$). The results suggest that extravasation of nanoparticles is dependent on the tumor vasculature, which has a high degree of variation that results in varying tumor extravasation. It is becoming widely accepted that only a selected population of patients with highly permeable tumors can benefit from nanomedicine [74–76], and a selection tool is needed to identify the receptive population.

3.2. Strategies to enhance the tumor extravasation of nanoparticles

3.2.1. Reduce particle size

Within the systemic circulation phase of drug delivery, the optimal particle size is about 100 nm, evading renal, hepatic and splenic filtration. However, the optimal particle size favoring tumor extravasation is not necessarily equivalent. Cabral et al. [77] compared the accumulation and effectiveness of differently sized long-circulating, drug-loaded polymeric micelles (diameters of 30, 50, 70 and 100 nm). In a hyperpermeable murine colon cancer model, there were no size-dependent restrictions on extravasation in tumors (all tumors exhibited a 10% ID uptake). In contrast, only particles smaller than 50 nm could penetrate poorly permeable hypovascular human pancreatic cancer models, with 30 nm particles fully inhibiting tumor growth and 50 nm particles inhibiting growth by only 50%. Particles above 50 nm had no inhibitory effect in this hypopermeable pancreatic model. Lee et al. [78] showed that accumulation of the 25 and 60 nm particles in the liver and spleen was not significantly different, but tumor uptake of the 25 nm particles was 2-fold higher relative to the 60 nm particles.

3.2.2. Tumor blood vessel modulating treatments

While hyperpermeable, the tortuous and chaotic vasculature of tumors represents a barrier to drug delivery because there is limited perfusion [65,79–81]. The process of angiogenesis is driven by factors released by tumor and stromal cells, and chief among the culprits is VEGF [82]. Blocking VEGF in tumors causes a reduction in the size and diameter of blood vessels with improved blood perfusion, leading to increased delivery of small molecule drugs [83,84]. Vascular normalization may enhance drug delivery for small molecules, but it can actually create barriers to nanomedicine therapy, as normalized blood vessels become less permeable to macromolecules, and the decrease in particle flux across the vessel walls may offset the benefits of increased perfusion [65]. Tanaka et al. [85] demonstrated enhancements

to EPR uptake by manipulation of vascular pressures with a prostaglandin analog (Beroprost): prostaglandin caused vasodilation, resulting in thinning of the already deformed tumor capillary wall, which in turn improved extravasation of macromolecules. Seki et al. [86] showed that nitroglycerin enhanced delivery of PEG-conjugated zinc protoporphyrin (PGP) and hence improved therapeutic efficacy via sustained EPR effect (more than 24 h). NO₂⁻ is first liberated from nitroglycerin and is then converted to NO under hypoxic conditions in cancer tissue, resulting in vasodilation and increased blood flow in the tumor, while NO₂⁻ production in normal tissue showed no significant increase. Seynhaeve et al. [86] demonstrated that the addition of low-dose tumor necrosis factor- α (TNF- α), which is a pro-inflammatory cytokine with known vascular permeabilizing activity, to systemic injections with PEGylated liposomes augmented tumor accumulation of these liposomes by 5- to 6-fold, which strongly correlated with enhanced tumor response. Seki et al. [87,88] showed that TNF- α can enhance the delivery of viral particles into tumors through a Rho A/Rho kinase dependent mechanism. TNF- α , however, is poorly tolerated when administered systemically, and therefore locoregional setups, such as isolated-limb-perfusion, are needed to exploit their beneficial effects. If such setups are available, the combination of extravasation-enhancing pretreatment with nanomedicine treatment can lead to significant increases in therapeutic efficacy [74]. Kano et al. [89] discovered that pre-treatment with a low dose of a TGF- β inhibitor (LY364947) decreased pericyte coverage of the tumor endothelium, leading to increased vascular permeability to nanoparticles.

Radiation treatment is also known to increase vascular permeability of solid tumors, and enhances the delivery of nanoparticles [90,91]. Li et al. [91] treated an OCa-1 ovarian carcinoma model with 5–15 Gy radiation followed by native paclitaxel and PG-TXL (polyglutamate conjugate of paclitaxel). Radiation significantly elevated VEGF levels, increased tumor vascular permeability by 26%, and improved tumor extravasation of PG-TXL by ~30%, but this result is not found with native paclitaxel. Davies et al. [90] reported similar results in an osteosarcoma xenograft model: they administered Caelyx (liposomal doxorubicin) in control and irradiated mice, and observed improved drug delivery in the irradiated mice and 60–70% efficacy enhancements. They further characterized the tumors with MRI, and demonstrated that radiation treatment enhanced perfusion significantly, an effect independent of drug treatment. Ionizing radiation generates reactive oxygen species (ROS) in DNA, resulting in tissue injury, including endothelial cell damage, with an increase in vascular permeability, edema, and fibrin accumulation in the extracellular matrix [92].

3.3. Factors affecting tumor retention of nanoparticles

Another aspect influencing delivery of nanoparticles is the retention effect arising from impaired or absent lymphatic drainage in tumors. It has been observed that elongated objects exhibit enhanced tissue retention following extravasation: Park et al. [93] demonstrated that dextran-coated nanochains and spheres (length ~50 nm) both extravasated into tumor tissue, but 48 h after injection the spheres had largely returned to the circulation, whereas the injected chains were better retained. Size also impacts retention in the tumor tissue: Torchilin et al. [94] demonstrated that the 10 nm micelles permeated into the tumor within 30 min post-injection, but the dose was not stably retained, with only 1/4 of the dose remaining in the tumor in 2 h. When the micelles were labeled with a 2C5 antibody, the tumor retention was significantly improved, with >80% of the dose retaining in the tumor in 2 h. Their data suggests a decreased retention effect for smaller (10 nm) particles, which can be reversed through the use of a targeting ligand.

4. Tumor penetration of nanoparticles and drug release

Nanoparticles that successfully extravasate into tumor tissues face another barrier consisting of high interstitial fluid pressure, dense stromal tissue, and complex interactions with macrophages, fibroblasts, and

tumor cells. BD analysis typically involves measurement of gross drug content in tissues, but is increasingly becoming a process of measuring where the particles are within tissues. The third phase of drug delivery involves nanoparticle penetration in the tumor tissue and drug release from nanoparticles.

4.1. Tumor physiological factors that impact nanoparticle penetration

4.1.1. Abnormal and heterogeneous vasculature

Tumor vasculature is highly irregular compared to that in normal tissues, with characteristics such as heterogeneous spatial distribution and uneven perfusion and permeability (reviewed in [65]). Tumor periphery is highly perfused, but vascular permeability is lower compared to the hypoxic core, wherein the reverse is observed [95]. Yuan et al. [30] prepared human adenocarcinoma xenografts in a dorsal window chamber model, permitting visualization of tumor vasculature and penetration of labeled liposomes. Compared to normal tissue, the liposomes exhibited significant accumulation in the adenocarcinoma, but did not distribute homogeneously: liposomes accumulated in perivascular clusters. Lee et al. [96] compared the intratumoral distribution of ¹¹¹In labeled polymeric micelles in MCF-7 and MDA-MB-468 tumors using MicroSPECT imaging, demonstrating a similar pattern of heterogeneous distribution. In both studies, nanoparticle uptake occurred mainly in the perfused tumor periphery, suggesting perfusion rather than permeability is the limiting factor for tumor penetration of nanoparticles.

4.1.2. Interstitial fluid pressure (IFP)

While tumor vasculature is often permeable to nanoparticles, further penetration into the tumor tissue depends on convective flow. In normal tissues, there is a net negative pressure drop between the blood vessel and the interstitial space, leading to fluid movement into the interstitial space and ultimately onwards to lymphatic ducts. However, as a result of abnormal permeability, lymphatic vessel malfunction, interstitial fibrosis, contraction of interstitial tissues mediated by stromal fibroblasts [86], and compression from multiplying tumor cells [97], interstitial fluid pressure (IFP) in tumors is increased and can be up to 60 mmHg [86,98–101]. High IFP disrupts normal convective flow, and large molecules and particles that rely on convective flow will not efficiently transport into the tumor compartment [102]. For nanoparticles, extravasation into the tumor periphery may be favored by increased permeability and perfusion, but movement to sites distant from the blood vessels is impaired by high IFP [77,96,103].

4.1.3. Stromal density

Cancer cells are surrounded by basement membrane, fibroblasts, immune cells, and extracellular matrix (ECM), which are collectively termed stroma, and is the dominant fraction of the total tumor mass [104,105]. The interaction between the tumor and stromal cells has been characterized as a wound that does not heal, given the inflammation and matrix building activity [104,106], but unlike normal tissue healing processes, fibroblasts in tumors are unregulated, continuously proliferate, and do not senesce [107]. The extracellular matrix produced by the activated fibroblast is a barrier to convective and diffusive transport, and this is particularly significant for nanoparticles compared to small molecules [106,108,109]. Furthermore, fibroblasts in the stromal tissues generate contractile forces, which increases IFP and reduces perfusion, further inhibiting drug transport and penetration [105]. In studies of nanoparticle penetration, Jain et al. [65] have demonstrated that the dense network of collagen fibers (ECM) prevents intratumoral transport, confining nanoparticles to the perivascular regions of the tumor.

4.1.4. Tumor associated macrophage (TAM)

Tumor tissue is rich in macrophage, with these populations reaching up to 60% of cells in some tumors [110,111]. Tumor associated macrophage (TAM) are well studied in their distinct role in immune

526 suppression, growth promotion, and metastases (refer to review [112]).
 527 TAMs have been shown to influence transport and drug release from
 528 nanoparticles [113–115]. Opaxio is a polyglutamate-paclitaxel conju-
 529 gate (PG-TXL), and studies with radiolabeled drug revealed that the
 530 drug metabolites were predominantly located within TAMs, whereas
 531 level of drug metabolite in tumor cells was 100–1000× less [113].
 532 Furthermore, the intratumoral distribution of PG-DTPA-Gd (a MR
 533 contrasted version of the polymer) was overlaid with TAMs, particularly
 534 in necrotic area of tumor, suggesting that TAMs were taking up PG and
 535 transporting the drug within the tumor [114]. A similar finding on
 536 TAM-related biofate was made with IT-101, a cyclodextrin conjugate
 537 of camptothecin. In *in vivo* models of glioblastoma, it was shown that
 538 microglia (a TAM) and lymphocytes were the predominant cell-types
 539 taking up IT-101, with microglia being particularly aggressive on the up-
 540 take [115]. Similar to the PG-TXL study, microglia was responsible for
 541 transporting the nanoparticles from the periphery into the tumor center
 542 within 1 day [71,115].

543 4.2. Nanoparticle properties that impact the tumor penetration

544 4.2.1. Size

545 Lee et al. [78,96] have demonstrated that tumor penetration of the
 546 25-nm particles from the vascular structures into the tumor tissue was
 547 doubled compared to the 60-nm particles (20 μm versus 46 μm from
 548 the nearest blood vessel). Moreover, particles >60 nm in diameter did
 549 not penetrate owing to the density of the collagen network [116]. Sev-
 550 eral studies, however, demonstrated that peak tumor penetration dif-
 551 fers for particles with different sizes, and that larger particles can
 552 indeed achieve similar tumor penetration as smaller molecules over
 553 an extended time frame [78,117].

554 4.2.2. Zeta potential

555 Neutral (± 10 mV) nanoparticles traveled up to three times more
 556 distance than charged analogs, and distributed more homogeneously
 557 within tissue: cationic materials tend to interact with negatively charged
 558 matrix polymers such as hyaluronan, and anionic materials tend to in-
 559 teract with positively charged matrix such as collagen [118,119], and
 560 these interactions impede transport. Nomura et al. [120] determined
 561 that liposomes carrying a nearly neutral charge (-2 to -5 mV) were
 562 able to penetrate through tumor tissue 14 time more rapidly compared
 563 to positively charge liposomes ($+48$ mV), which barely migrated at all.
 564 Similarly, Stylianopoulos et al. [118] demonstrated by modeling and ex-
 565 perimental validation that highly positive particles exhibited reduced
 566 penetration and distributed less homogeneously. Lieleg et al. [119] stud-
 567 ied the penetration of charged polystyrene and liposomes in matrix, and
 568 found that when the zeta potential was below -20 mV or above 10 mV,
 569 their diffusion coefficients were orders of magnitudes lower than values
 570 for neutral particles.

571 4.2.3. Targeting ligands

572 Lee et al. [78] showed that the 25 nm EGFR-targeted block copoly-
 573 mer micelles exhibited reduced tumor penetration ($D_{\text{mean}} = 29 \mu\text{m}$)
 574 compared to the non-targeted micelles ($D_{\text{mean}} = 42 \mu\text{m}$) due to the
 575 “binding site barrier” effect, where specific binding and/or cellular inter-
 576 nalization of antibodies by the targeted cells halts their penetration in
 577 solid tumors. This barrier effect was not observed for the 60 nm version
 578 of the nanoparticles, as particle penetration was already limited
 579 ($\sim 20 \mu\text{m}$) by matrix interactions related to size.

580 4.3. Approaches to modulate tumor penetration of therapeutic agents

581 4.3.1. IFP reduction

582 Reducing IFP to restore a normalized flow pattern is anticipated to
 583 enhance convective transport and intratumoral penetration of thera-
 584 peutic agents. However, the majority of the studies were performed
 585 with small molecules [121,122], and the relevance to nanoparticles is

yet to be confirmed. In the first type of approach, tumor vasculature is
 586 normalized by treatment with anti-angiogenic drugs which target
 587 VEGF, including drugs such as bevacizumab, and cediranib [65,80,123],
 588 and which results in lower IFP. In a second approach to IFP reduction,
 589 stromal fibroblasts are targeted. Prostaglandins interact with fibroblasts
 590 to increase contractile forces and therefore raise IFP. Pietras et al.
 591 [124,125] demonstrated that treatment with a prostaglandin inhibitor
 592 such as Imatinib reduced IFP and improved small molecule drug deliv-
 593 ery within the tumor microenvironment by 1.8-fold. In a third ap-
 594 proach, IFP can be reduced by debulking the ECM or stromal cells.
 595 Treatment with of ECM with ECM-degrading enzymes such as hyal-
 596 uronidase or collagenase, or debulking tumors cells with drugs such as
 597 paclitaxel can reduce IFP and enhance transport of chemotherapeutics
 598 by 4- and 2-fold, respectively [126].
 599

4.3.2. Stromal depletion

600 There is current interest in targeting stroma with molecules or
 601 nanoparticles, and fibroblasts in particular are identified as good targets,
 602 to debulk the tumor, reduce tumorigenic stimuli, alleviate high IFP, and
 603 restore perfusion and drug delivery [128]. Most recently, Murakami et al.
 604 [127] demonstrated that their nanoparticles composed of PEGylated and
 605 acetylated carboxymethylcellulose with docetaxel interacted selectively
 606 with cancer associated fibroblasts (CAFs) in the breast tumor models
 607 (Fig. 4). Greater than 85% of the nanoparticles were internalized by
 608 CAFs in the tumor microenvironment possibly via an albumin-SPARC
 609 (secreted protein acidic and rich in cysteine) dependent mechanism.
 610 SPARC is a tissue remodeling molecule produced at high concentrations
 611 by tumor stromal cells. This interaction led to almost complete depletion
 612 of CAFs within a week, with 70-fold increased tumor perfusion, 50% re-
 613 duction in ECM and IFP, and >10-fold decrease in metastases. Whether
 614 this nanoparticle treatment can increase subsequent delivery of other
 615 drugs or macromolecules is yet to be studied. Several approaches to
 616 stromal depletion are being tested in clinical trials, including Abraxane
 617 (paclitaxel-albumin nanoparticle) and Hedgehog inhibitors [129,130].
 618 In clinical evaluation in combination with gemcitabine, Abraxane
 619 (Nab-paclitaxel) reduced pancreatic ECM, possibly due to increased in-
 620 teractions with the stroma cells via a SPARC-mediated mechanism.
 621 This combination treatment resulted in 3.7-fold increased delivery of
 622 gemcitabine into the debulked xenografted tumor [129]. Loeffler et al.
 623 [131] showed that fibroblast activation protein (FAP)-vaccinated mice
 624 displayed decreased collagen type I expression in the tumor, and as stro-
 625 ma was accordingly less dense, the tumor uptake of doxorubicin was in-
 626 creased up to 70%. They also demonstrated similar effects with
 627 fluorescein and albumin, suggesting the stromal depletion strategy
 628 may be applied to enhance the delivery of both small molecules and
 629 macromolecules.
 630

4.4. Drug release from nanoparticles

631 As particles extravasate into the tumor, there must be either intersti-
 632 tial drug release, or internalization of the particles and intracellular re-
 633 lease to exert pharmacological effects: composition of the nanoparticles
 634 must therefore accommodate mechanisms for drug release, preferably
 635 sustained release. Two clinical examples (Doxil and SPI-077) illustrate
 636 the challenge associated with excessive stability. Doxil delivers 10 to
 637 15 times more doxorubicin to the tumor compared to standard therapy,
 638 but Doxil in the tumor has low bioavailability (40–50%) due to slow re-
 639 lease, and as a result, efficacy enhancements are modest [132–134]. Sim-
 640 ilarly, SPI-077 (a liposomal formulation of cisplatin) exhibited significant
 641 tumor accumulation but no antitumor effect. Analysis revealed that cis-
 642 platin is membrane impermeable, and was retained inside the stable li-
 643 posomes and not bioavailable [132,135].
 644

645 Conversely, a formulation can exhibit excessive instability, and in
 646 the field of taxane therapies, this is a persistent challenge. Taxanes
 647 have been formulated into polymeric micelles such as Genexol [136]
 648 and NK105 [137], and while these technologies enhance efficacy, the

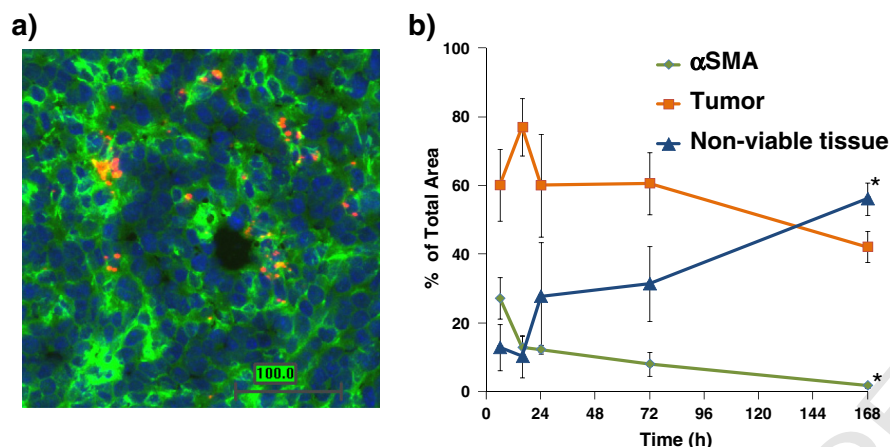


Fig. 4. Cellax nanoparticles target cancer-associated fibroblasts. (a) Balb/c mice bearing 4T1 breast tumors were treated with fluorescently labeled Cellax particles (red), and α -SMA + CAF were immunostained with FITC (green). Definiens image analysis of tumors for total area (defined by DAPI nuclear staining), α -SMA content (green) and Cellax-Dil (red) demonstrated that 85% of the Cellax particles were associated with α -SMA + CAF. Cellax-treated 4T1 tumors were analyzed to quantify different cell populations in the tumors over a time course (b): subsequent to therapy, α -SMA content dropped rapidly over 16 h, followed by a steady decrease over 168 h. Tumor cells as a percentage of total tumor area did not undergo a significant decline in the 168 h timeframe, whereas non-viable tissue increased significantly, suggesting that the decline of α -SMA + cells is the primary therapeutic effect. Adapted from ref [127].

taxanes rapidly partition out of the polymeric micelles and bind with serum proteins during blood circulation, and the PK improvement over the standard formulations (Taxol or Taxotere) is not significant in human patients [136,138,139]. In the Abraxane formulation, human serum albumin is complexed with paclitaxel to form 130-nm particles, and likewise, while efficacy enhancements are observed due to an increase in the tolerated dose, the PK profile of the paclitaxel is unchanged [70,140–142]. Opaxio is a conjugate of paclitaxel and polyglutamate, and while positive results in Phase I and II were reported and PK parameters were significantly enhanced [143], the hallmark taxane side effects of neutropenia persisted, and it failed to enhance efficacy in Phase III. In preclinical evaluation it was observed that Opaxio decomposed during circulation, forming polymeric fragments of taxane that distributed to many normal organs to a significant extent [144]. It may be that Opaxio is not stable enough to minimize toxicity and leverage the EPR effect to the full advantage. The challenge then is to maintain stability to achieve improved PK profiles, while providing for a release mechanism inside the tumor.

4.5. Factors impacting cellular internalization of nanoparticles and the drug release

4.5.1. Mechanisms of cellular internalization of nanoparticles

There are two major endocytic mechanisms by which cells take up particles and macromolecules, and these are referred to as phagocytosis and pinocytosis [145]. Large particles ($>1 \mu\text{m}$) are generally internalized by phagocytosis mechanisms, which are present only on professional phagocytic cells, such as macrophages, neutrophils, or dendritic cells [146]. Therefore pinocytosis is more relevant to cellular uptake of nanoparticles and can occur either *via* adsorptive pinocytosis or *via* receptor-mediated endocytosis [147]. Pinocytic mechanisms of uptake can be further divided into caveolae-mediated endocytosis ($\sim 60 \text{ nm}$) or clathrin-mediated endocytosis ($\sim 120 \text{ nm}$), as well as clathrin-independent or caveolin-independent endocytosis ($\sim 90 \text{ nm}$) [146]. The details of the exact mode of endocytosis are important because they determine the path of trafficking through various possible subcellular compartments. For example, nanoparticles internalized through clathrin-mediated endocytosis are destined for a lysosomal compartment, whereas those internalized through a caveolin-mediated process are not. In clathrin-mediated endocytosis internalization, endosomal escape must occur before fusion with a lysosome to prevent degradation of the cargo under harsh lysosomal conditions. In either case, endosomal escape is usually necessary to allow access of the carrier to the desired subcellular compartment. Ligands such as folic acid, albumin and

cholesterol conjugated to the surface of engineered nanoparticles can facilitate uptake through caveolin-mediated endocytosis, whereas ligands for glycoreceptors promote clathrin-mediated endocytosis. Alternatively, macropinocytosis, a non-caveolin-mediated, non-clathrin-mediated process, can be engaged by incorporating cell-penetrating peptides, such as a trans-activating transcriptional activator (TaT) peptide into the design of engineered nanoparticles. For a nanoparticle entering the lysosomal compartments, drug release can be engineered to occur *via* hydrolysis of sensitive functional groups (such as an ester): the released drug must be reasonably resistant to the lysosomal environment and be able to escape into the cytosol [148–150].

4.5.2. Size

Nanoparticle size is a key parameter affecting the cellular uptake rate as it influences their internalization mechanism. In general, particles in the 40–200 nm range exhibit cellular uptake *in vitro* [151,152]. Gratton et al. [152] examined the uptake of hydrogel particles ranging from 1 to 200 nm in diameter in HeLa cells, and found that very small (1 nm) and larger (150–200 nm) particles were readily internalized. Jiang et al. [153] investigated the size-dependent binding and uptake of the transtuzumab-conjugated nanoparticles (2–100 nm) with ErbB2+ cells and found that 40–50 nm particles exhibited the highest amount of cellular internalization, which may be due to the optimal antibody density on the particle surface that triggers maximal cross-linking of the membrane receptors.

4.5.3. Shape

Gratton et al. [152] designed a series of cationic cross-linked PEG-based hydrogels of varying sizes and shapes *via* a top-down lithographic fabrication method (PRINT: Particle Replication In Non-wetting Templates) and examined the cellular internalization pathways using HeLa cells. Nonspherical particles with dimensions as large as 3 μm were easily internalized by using several different mechanisms of endocytosis. Similar findings demonstrate the enhanced internalization of nonspherical particles over their spherical counterparts for nanosized rod-like biodegradable mesoporous silica nanoparticles [154] and iron oxide nanoworms [93]. On the contrary, several other studies have found that the spherical forms of gold nanoparticles [155] and polymeric nanoparticles [156] were internalized to a greater extent than their corresponding nonspherical particles. For example, cells took up 5 and 4-fold more 74 and 14 nm spherical gold nanoparticles than 74 \times 14 nm rod-shaped gold nanoparticles, respectively [155]. Nevertheless, shape of particles not only affects tumor cell internalization but also determines the interaction with RES, and the PK and tumor retention as discussed in the previous sections.

733 Impacts of shape in the three phases of delivery should be comprehen- 796
734 sively considered when designing nanoparticles. 797

735 4.5.4. PEGylation 798

736 To reduce opsonization by blood proteins and clearance by RES, hy- 800
737 drophilic stealth polymers (e.g., PEG) have been used as a surface coat- 801
738 ing material. PEG, however, may be an obstacle and hinder to 802
739 interaction with target cells, resulting in reduced efficacy. Several differ- 803
740 ent approaches have been made to remove the PEG coating after the 804
741 particle arrives at the target site. Guo et al. [157] prepared a removable 805
742 PEG coating which stabilizes the fusogenic DOPE in liposomes at neutral 806
743 pH. PEG was linked to DOPE *via* a diorthoester bond, and hydrolysis of 807
744 the conjugation at the low endosomal pH in the range of 5–6 occurred 808
745 within 1 h, leading to particle fusion with the endosomal membrane 809
746 and release of contents into the cytosol. A similar strategy was applied 810
747 to TAT-liposomes masked with a cleavable PEG coating: the PEG chains 811
748 were released at the acidic pH (pH 5–6), exposing the TAT peptides to 812
749 interact and enhance internalization by the targeted cancer cells [158]. 813
750 Similarly, the same group shielded the TAT-liposomes with a long- 814
751 chain PEG, which was conjugated to the liposomal surface *via* a MMP2 815
752 cleavable peptide (Gly-Pro-Leu-Gly-Ile-Ala-Gly-Gln) [159]. They report- 816
753 ed that the liposomes were de-PEGylated by the extracellular MMP2 in 817
754 the tumor cells, exposing the TAT peptide on the nanoparticle surface 818
755 for increased cellular uptake. MacLachlan's group [160] developed stabi- 819
756 lized nucleic acid lipid particles (SNALP) consisting of a siRNA encapsu- 820
757 lated in an ionizable lipid bilayer (pKa ~6) with a PEGylated lipid. They 821
758 found that when the carbon chain length of the PEGylated lipid was 822
759 shortened from C20 to C14, the blood circulation time was decreased, 823
760 but accompanied with increased hepatocellular uptake of the formula- 824
761 tion, enhanced gene silencing activity in the liver, and reduced cytokine 825
762 stimulation. The PEGylated lipid with a shortened carbon chain is diffu- 826
763 sive, and readily leaves the lipid bilayer during blood circulation to facili- 827
764 tate binding of Apo E to the naked SNALP, which in turn recognizes Apo 828
765 E and LDL receptors on the hepatocytes, therefore triggering endocyto- 829
766 sis. In the acidic endosomal and lysosomal environment, SNALP is ion- 830
767 ized and becomes cationic to interact with the negatively charged lipid 831
768 membrane, promoting siRNA to escape into the cytosol, the site of ac- 832
769 tion. On the other hand, SNALP prepared with long acyl chain PEGylated 833
770 lipids remain stable in the blood circulation, and have an increased 834
771 probability of interacting with immune cells, inducing enhanced proin- 835
772 flammatory cytokine production. 836

773 4.5.5. Zeta potential 837

774 Cationic nanoparticles are generally known to exhibit increased up- 838
775 take by cells *via* the charge–charge interaction mediated adsorptive en- 839
776 docytosis compared to neutral and anionic particles [161–163]. Again, 840
777 the PK of the charged nanoparticle has to be considered, as charged 841
778 nanoparticles often display increased interaction with serum proteins, 842
779 resulting in accelerated blood clearance compared to neutral particles. 843
780 As just discussed, it is feasible to design nanoparticles that shed PEG- 844
781 shielding after tumor extravasation in order to expose cationic particles 845
782 that can interact with target cells [164,165]. In a slightly different variant 846
783 of this approach, Choi et al. [166] formulated poly(ethyleneglycol)- 847
784 diorthoester-distearoylglycerol lipid (POD) stabilized plasma lipid 848
785 nanoparticles (SPLP): POD-SPLP contain 13 wt.% PEG: the PEG brush 849
786 dissipated at pH 5.3 within 110 min, exposing a cationic particle. Both 850
787 the POD-SPLP and PEG-SPLP were internalized to a qualitatively similar 851
788 extent within 2 h of incubation but gene transfer increased up to 3 or- 852
789 ders of magnitude with POD-SPLP, due to more rapid escape of plasmid 853
790 DNA from the endosome. 854

791 4.5.6. Targeting ligands 855

792 A commonly used strategy for improving bioavailability of nano- 856
793 particles in a tumor is to conjugate a targeting ligand, allowing the 857
794 binding with the surface receptor on the tumor cells, triggering 858
795 receptor-mediated endocytosis for increased intracellular delivery of a

796 drug. Although success has been reported for many nanoparticle 797
798 systems and animal models, this approach suffers from the following 799
799 disadvantages: first, cellular internalization happens only after extrava- 800
800 sation of nanoparticles, and the cellular uptake only occurs around the 801
801 microvessels, resulting in limited tumor penetration and heterogeneous 802
802 drug uptake [3]. As discussed earlier, Lee et al. [78] demonstrated that 803
803 the targeted nanoparticles display restricted penetration compared to 804
804 non-targeted particles; second, some ligand-conjugated nanoparticles, 805
805 including antibody- [167] or small molecule-decorated nanoparticles 806
806 [168,169] display enhanced blood clearance, reducing the tumor accu- 807
807 mulation; third, cellular internalization by receptor-mediated endocyto- 808
808 sis leads to drug decomposition in the endosome/lysosome [170]. 809
809 Therefore, targeted nanoparticles do not always exhibit improved ther- 810
810 apy compared to the non-targeted ones [132]. 811

812 Another important point to note is that conjugating a tumor- 813
813 selective ligand onto nanoparticles does not improve the specificity of 814
814 tissue distribution, which is mainly determined by nanoparticle physi- 815
815 cochemical properties, and the ligand only sees the antigen after nano- 816
816 particle extravasation. Using proton emission tomography/computed 817
817 tomography (PET/CT), Bartlett et al. [171,172] compared the biological 818
818 activity of siRNA payloads in tumors delivered *via* non-targeted and 819
819 transferrin conjugated nanoparticles. They found no difference in BD 820
820 between the targeted and the non-targeted nanocomplexes, while in- 821
821 creased gene silencing activity was seen with the targeted complex. 822
822 The authors concluded that the primary function of the ligand was not 823
823 in targeting the complexes to the tumor tissue, but to increase the intra- 824
824 cellular uptake. Similar results have been reported by other groups 825
825 [167,173]. 826

827 4.5.7. TAM content and drug release 830

831 Zamboni et al. [174] have shown that drug release of a camptothecin 832
832 analog from the PEGylated liposomes was more efficient in tumors 833
833 characterized by higher macrophage content. For example: $4.9 \pm 3.0\%$ 834
834 of SKOV-3 tumors stained positive for TAM, whereas only $1.1 \pm 0.7\%$ 835
835 in A375 tumor. While the total drug accumulation in the tumor tissues 836
836 was similar ($13\text{--}16 \mu\text{g}/\text{mL h}$), release of camptothecin in the extracellu- 837
837 lar fluid was 2-fold higher in the TAM-rich SKOV-3 tumors. The data 838
838 suggest that TAM not only is active in phagocytosing nanoparticles, 839
839 but also efficient in digesting nanoparticles and facilitating drug release. 840
840 However, whether TAM content can be a biomarker to correlate drug 841
841 release from nanoparticles and their efficacy needs to be validated. 842

843 5. Conclusion and perspectives 846

847 There is a continuum of biological barriers to effective drug delivery 848
848 by nanoparticles (Fig. 1), ranging from the RES interaction with 849
849 nanoparticles, to the extravasation of nanoparticles into highly perme- 850
850 able tumor tissues, and penetration of nanoparticles through the stroma 851
851 and ultimate drug release around or inside the target cells. There are 852
852 conflicting design parameters as a result of this multi-system interac- 853
853 tion, especially in optimal size. Approved cancer nanomedicines (Doxil, 854
854 DaunoXome, Abraxane and Marqibo) are 80–130 nm in diameter. How- 855
855 ever, there is increasing interest in developing small particles (<50 nm) 856
856 exhibiting improved tumor permeability and penetration. 857

858 PEGylation has been employed in many nanoparticles to reduce the 859
859 RES interaction and prolong the blood circulation. Nevertheless, the RES 860
860 is still responsible for clearing majority of nanoparticles, typically leav- 861
861 ing <10% ID/g delivered to the tumors [3,132]. There are limits to how 862
862 much PEG can be integrated into a nanoparticle before it destabilizes 863
863 the structure. The Huang lab [175,176] has demonstrated in their LPD 864
864 (lipid-polycation-DNA) and LCP (lipid-calcium phosphate) nanoparticle 865
865 systems that >10 mol% of DSPE-PEG₂₀₀₀ could be introduced to the lipid 866
866 membranes that are stabilized by charge–charge interaction. These 867
867 highly PEGylated LPD and LCP nanoparticles displayed minimal RES 868
868 clearance in the liver (~10% ID), a clear differentiation from many 869
869 other nanoparticles. However, PEGylation has been shown to reduce 870

nanoparticle interaction with target cells, and is responsible for immune response, especially when an immunostimulatory agent is carried, such as pDNA and siRNA. A variety of strategies have been developed to facilitate de-PEGylation of nanoparticles to reduce the immunotoxicity or cellular bioavailability. Developing a PEG alternative to shield nanoparticles from RES recognition remains an open challenge.

Clinical tumors possess a high degree of variation in vasculature, which impacts nanoparticle extravasation and the intratumoral distribution, leading to varying therapeutic activities among patients [75,76]. Patient characteristics (e.g., age, gender, tumor type, tumor location, body composition and prior treatments) can also affect the EPR effect of nanomedicine [177]. Additionally, the EPR effect is mainly observed with large solid tumors, and whether this effect applies to small metastases needs to be validated in a large number of patients. To improve therapeutic outcomes, a selection tool needs to be developed to stratify patients into candidates and non-candidates for nanomedicine therapy. A nanoparticle can be manufactured with multiple functions, delivering both drug and imaging agents, enabling real-time and non-invasive measurement of PK, BD and tumor delivery of the nanoparticles. In future, cancer patients could then be screened for treatment suitability using multifunctional nanoparticles and the corresponding imaging technologies. Karathanasis et al. [178] screened mouse breast cancer models with an injectable liposomal probe containing iodine to identify which subgroups were good candidates for nanoparticle therapy, and demonstrated excellent correlation ($R^2 = 0.838$) between SPECT measurements and therapeutic response to the liposomal doxorubicin. Ideally, a general method utilizing a contrast agent and MRI can be developed to screen the prevalence of the EPR effect in human tumors and to stratify patients for receiving nanotherapeutics.

The issue of low drug bioavailability exemplified by Doxil and SPI-077 (PEGylated liposomal cisplatin) is a significant concern in the design of nanoparticles. The development of triggered-release nanoparticles, which release drug locally in the tumor, achieves improved bioavailability while reducing systemic exposure. The most advanced triggered release technology is the hyperthermia-activated liposomal formulation, a nanoparticle that burst-releases 100% drug content at 41–42 °C within 20 s, but is relatively stable at 37 °C [179–183]. In combination with image-guided heating technologies, the drug can be released intravascularly within the locally heated tumor, generating a high drug concentration gradient for improved delivery and tumor penetration of bioavailable drug. This EPR-effect-independent nanotechnology is being tested in clinical trials. The design of nanoparticles capable of controlled release in the tumor compartment remains an area of pursuit in the field [148–150]. It is also suggested that more research should be directed towards development of new types of nanoparticle delivery systems that do not rely on the EPR effect.

While ligand targeted therapies are experiencing some success, an effective interaction between a ligand and the tumor cell can occur only after the targeted nanoparticles have evaded the RES clearance, extravasated into the tumor tissue and penetrated through the ECM and stroma [65,78]. Due to the difficulty in targeting tumor cells, specific receptors on endothelium within tumors are attractive targets as they present to the bloodstream and circulating nanoparticles [184]. The most commonly utilized ligand is RGD, a peptide recognized by integrins overexpressed on angiogenic endothelial cells [116]. Recently, the Ruoslahti group [118] developed a tumor penetrating peptide, iRGD (CRGDK/RGPD/EC): iRGD targets the integrins on tumor vascular endothelial cells with the RGD motif, and then the peptide is digested to expose RGDK/R, which binds to NRP-1 and induces vascular and tissue permeabilization. Conjugation or co-injection of iRGD with a macromolecule significantly improved the tumor delivery by >7-fold.

In the past few decades, the nanomedicine research has been focused on optimizing the physicochemical parameters of nanoparticles (size, shape, surface charge, ligand, release rate) to obtain optimal PK and delivery. Current research is emphasizing on improving understanding of how human physiology and tumor biology affect PK, BD

and intratumoral penetration of nanoparticles. Various approaches have been investigated to modulate the tumor microenvironment to allow increased extravasation of nanoparticles, including modulating the vascular dynamics (blood flow, pressure and permeability), and debulking the tumor by depleting the stromal component (CAFs, ECM). It is now believed that both optimization of the nanoparticles and the tumor microenvironment are required for optimal delivery [75]. Currently, the field of research is still focused on addressing the permeability part of the EPR equation with less emphasis on the retention aspect, which is driven by the impaired lymphatic drainage in the tumor. More functional imaging technologies with quantitative capabilities should be developed to study the lymphatic function in the tumor, and how this parameter impacts IFP, nanoparticle penetration and retention. With gains in fundamental knowledge, rational design of an optimal nanomedicine can then be realized to achieve the maximized therapeutic effect in image-stratified patients.

Acknowledgment

The authors acknowledge the following funding agencies: the Ontario Institute for Cancer Research, MaRS Innovation, the Ontario Centres of Excellence, the Canadian Institutes of Health Research, the Prostate Cancer Foundation, and the National Institutes of Health.

References

- [1] J. Fang, H. Nakamura, H. Maeda, The EPR effect: unique features of tumor blood vessels for drug delivery, factors involved, and limitations and augmentation of the effect, *Adv. Drug Deliv. Rev.* 63 (2011) 136–151.
- [2] J. Fang, T. Sawa, H. Maeda, Factors and mechanism of “EPR” effect and the enhanced antitumor effects of macromolecular drugs including SMANCS, *Adv. Exp. Med. Biol.* 519 (2003) 29–49.
- [3] S.D. Li, L. Huang, Pharmacokinetics and biodistribution of nanoparticles, *Mol. Pharm.* 5 (2008) 496–504.
- [4] D. Liu, A. Mori, L. Huang, Role of liposome size and RES blockade in controlling biodistribution and tumor uptake of GM1-containing liposomes, *Biochim. Biophys. Acta* 1104 (1992) 95–101.
- [5] S.M. Moghimi, A.C. Hunter, Capture of stealth nanoparticles by the body's defences, *Crit. Rev. Ther. Drug Carrier Syst.* 18 (2001) 527–550.
- [6] P. Opanasopit, M. Nishikawa, M. Hashida, Factors affecting drug and gene delivery: effects of interaction with blood components, *Crit. Rev. Ther. Drug Carrier Syst.* 19 (2002) 191–233.
- [7] S. Nagayama, K. Ogawara, Y. Fukuoka, K. Higaki, T. Kimura, Time-dependent changes in opsonin amount associated on nanoparticles alter their hepatic uptake characteristics, *Int. J. Pharm.* 342 (2007) 215–221.
- [8] H. Otsuka, Y. Nagasaki, K. Kataoka, PEGylated nanoparticles for biological and pharmaceutical applications, *Adv. Drug Deliv. Rev.* 55 (2003) 403–419.
- [9] Y. Sadzuka, S. Hirotsu, S. Hirota, Effect of liposomalization on the antitumor activity, side-effects and tissue distribution of CPT-11, *Cancer Lett.* 127 (1998) 99–106.
- [10] P. Crosasso, M. Ceruti, P. Brusa, S. Arpicco, F. Dosio, L. Cattel, Preparation, characterization and properties of sterically stabilized paclitaxel-containing liposomes, *J. Control. Release* 63 (2000) 19–30.
- [11] W.L. Lu, X.R. Qi, Q. Zhang, R.Y. Li, G.L. Wang, R.J. Zhang, S.L. Wei, A pegylated liposomal platform: pharmacokinetics, pharmacodynamics, and toxicity in mice using doxorubicin as a model drug, *J. Pharmacol. Sci.* 95 (2004) 381–389.
- [12] D.E. Owens III, N.A. Peppas, Opsonization, biodistribution, and pharmacokinetics of polymeric nanoparticles, *Int. J. Pharm.* 307 (2006) 93–102.
- [13] S.D. Perrault, C. Walkey, T. Jennings, H.C. Fischer, W.C. Chan, Mediating tumor targeting efficiency of nanoparticles through design, *Nano Lett.* 9 (2009) 1909–1915.
- [14] F. Alexis, E. Pridden, L.K. Molnar, O.C. Farokhzad, Factors affecting the clearance and biodistribution of polymeric nanoparticles, *Mol. Pharm.* 5 (2008) 505–515.
- [15] C. Fang, B. Shi, Y.Y. Pei, M.H. Hong, J. Wu, H.Z. Chen, *In vivo* tumor targeting of tumor necrosis factor- α -loaded stealth nanoparticles: effect of MePEG molecular weight and particle size, *Eur. J. Pharm. Sci.* 27 (2006) 27–36.
- [16] M.J. Ernsting, W.L. Tang, N.W. Maccallum, S.D. Li, Preclinical pharmacokinetic, biodistribution, and anti-cancer efficacy studies of a docetaxel-carboxymethylcellulose nanoparticle in mouse models, *Biomaterials* 33 (2012) 1445–1454.
- [17] C.D. Walkey, J.B. Olsen, H. Guo, A. Emili, W.C. Chan, Nanoparticle size and surface chemistry determine serum protein adsorption and macrophage uptake, *J. Am. Chem. Soc.* 134 (2012) 2139–2147.
- [18] N. Dos Santos, C. Allen, A.M. Doppen, M. Anantha, K.A. Cox, R.C. Gallagher, G. Karlsson, K. Edwards, G. Kenner, L. Samuels, M.S. Webb, M.B. Bally, Influence of poly(ethylene glycol) grafting density and polymer length on liposomes: relating plasma circulation lifetimes to protein binding, *Biochim. Biophys. Acta* 1768 (2007) 1367–1377.

- [19] A. Chanan-Khan, J. Szebeni, S. Savay, L. Liebes, N.M. Rafique, C.R. Alving, F.M. Muggia, Complement activation following first exposure to pegylated liposomal doxorubicin (Doxil): possible role in hypersensitivity reactions, *Ann. Oncol.* 14 (2003) 1430–1437.
- [20] J. Szebeni, Complement activation-related pseudoallergy: a new class of drug-induced acute immune toxicity, *Toxicology* 216 (2005) 106–121.
- [21] W.C. Chen, J.P. May, S.D. Li, Immune responses of therapeutic lipid nanoparticles, *Nanotechnol. Rev.* 2 (2013) 201–213.
- [22] T. Ishida, T. Ichikawa, M. Ichihara, Y. Sadzuka, H. Kiwada, Effect of the physico-chemical properties of initially injected liposomes on the clearance of subsequently injected PEGylated liposomes in mice, *J. Control. Release* 95 (2004) 403–412.
- [23] A. Judge, K. McClintock, J.R. Phelps, I. MacLachlan, Hypersensitivity and loss of disease site targeting caused by antibody responses to PEGylated liposomes, *Mol. Ther.* 13 (2006) 328–337.
- [24] M. Barz, R. Luxenhofer, R. Zentel, M.J. Vicent, Overcoming the PEG-addiction: well-defined alternatives to PEG, from structure–property relationships to better defined therapeutics, *Polym. Chem.* 2 (2011) 1900–1918.
- [25] R. Hoogenboom, Poly(2-oxazoline)s: a polymer class with numerous potential applications, *Angew. Chem. Int. Ed. Engl.* 48 (2009) 7978–7994.
- [26] M. Nahrendorf, E. Keliher, B. Marinelli, P. Waterman, P.F. Feruglio, L. Fexon, M. Pivovarov, F.K. Swirski, M.J. Pittet, C. Vinegoni, R. Weissleder, Hybrid PET–optical imaging using targeted probes, *Proc. Natl. Acad. Sci. U. S. A.* 107 (2010) 7910–7915.
- [27] C.H. Choi, C.A. Alabi, P. Webster, M.E. Davis, Mechanism of active targeting in solid tumors with transferrin-containing gold nanoparticles, *Proc. Natl. Acad. Sci. U. S. A.* 107 (2010) 1235–1240.
- [28] P.L. Rodriguez, T. Harada, D.A. Christian, D.A. Pantano, R.K. Tsai, D.E. Discher, Minimal “Self” peptides that inhibit phagocytic clearance and enhance delivery of nanoparticles, *Science* 339 (2013) 971–975.
- [29] H.S. Choi, W. Liu, P. Misra, E. Tanaka, J.P. Zimmer, B. Itty Ipe, M.G. Bawendi, J.V. Frangioni, Renal clearance of quantum dots, *Nat. Biotechnol.* 25 (2007) 1165–1170.
- [30] F. Yuan, M. Dellian, D. Fukumura, M. Leunig, D.A. Berk, V.P. Torchilin, R.K. Jain, Vascular permeability in a human tumor xenograft: molecular size dependence and cutoff size, *Cancer Res.* 55 (1995) 3752–3756.
- [31] L.T. Chen, L. Weiss, The role of the sinus wall in the passage of erythrocytes through the spleen, *Blood* 41 (1973) 529–537.
- [32] S.M. Moghimi, A.C. Hunter, J.C. Murray, Long-circulating and target-specific nanoparticles: theory to practice, *Pharmacol. Rev.* 53 (2001) 283–318.
- [33] J. Hrkach, D. Von Hoff, M.M. Ali, E. Andrianova, J. Auer, T. Campbell, D. De Witt, M. Figa, M. Figueiredo, A. Horhota, S. Low, K. McDonnell, E. Peeke, B. Retnarajan, A. Sabinis, E. Schnipper, J.J. Song, Y.H. Song, J. Summa, D. Tompsett, G. Troiano, T. Van Geen Hoven, J. Wright, P. Lorusso, P.W. Kantoff, N.H. Bander, C. Sweeney, O.C. Farokhzad, R. Langer, S. Zale, Preclinical development and clinical translation of a PSMA-targeted docetaxel nanoparticle with a differentiated pharmacological profile, *Sci. Transl. Med.* 4 (2012) 128ra139.
- [34] J.A. Champion, S. Mitragotri, Role of target geometry in phagocytosis, *Proc. Natl. Acad. Sci. U. S. A.* 103 (2006) 4930–4934.
- [35] J.A. Champion, S. Mitragotri, Shape induced inhibition of phagocytosis of polymer particles, *Pharm. Res.* 26 (2009) 244–249.
- [36] Y. Geng, P. Dalhaimer, S. Cai, R. Tsai, M. Tewari, T. Minko, D.E. Discher, Shape effects of filaments versus spherical particles in flow and drug delivery, *Nat. Nanotechnol.* 2 (2007) 249–255.
- [37] S. Li, J. Nickels, A.F. Palmer, Liposome-encapsulated actin-hemoglobin (LEAChb) artificial blood substitutes, *Biomaterials* 26 (2005) 3759–3769.
- [38] T. Cedervall, I. Lynch, M. Foy, T. Berggard, S.C. Donnelly, G. Cagney, S. Linse, K.A. Dawson, Detailed identification of plasma proteins adsorbed on copolymer nanoparticles, *Angew. Chem. Int. Ed. Engl.* 46 (2007) 5754–5756.
- [39] A. Gessner, R. Waicz, A. Lieske, B. Paulke, K. Mader, R.H. Muller, Nanoparticles with decreasing surface hydrophobicities: influence on plasma protein adsorption, *Int. J. Pharm.* 196 (2000) 245–249.
- [40] P.R. Cullis, A. Chonn, S.C. Semple, Interactions of liposomes and lipid-based carrier systems with blood proteins: relation to clearance behaviour *in vivo*, *Adv. Drug Deliv. Rev.* 32 (1998) 3–17.
- [41] A. Chonn, S.C. Semple, P.R. Cullis, Association of blood proteins with large unilamellar liposomes *in vivo*. Relation to circulation lifetimes, *J. Biol. Chem.* 267 (1992) 18759–18765.
- [42] S.M. Moghimi, H.M. Patel, Tissue specific opsonins for phagocytic cells and their different affinity for cholesterol-rich liposomes, *FEBS Lett.* 233 (1988) 143–147.
- [43] J. Senior, J.C. Crawley, G. Gregoriadis, Tissue distribution of liposomes exhibiting long half-lives in the circulation after intravenous injection, *Biochim. Biophys. Acta* 839 (1985) 1–8.
- [44] T.M. Allen, C. Hansen, Pharmacokinetics of stealth versus conventional liposomes: effect of dose, *Biochim. Biophys. Acta* 1068 (1991) 133–141.
- [45] D.C. Drummond, O. Meyer, K. Hong, D.B. Kirpotin, D. Papahadjopoulos, Optimizing liposomes for delivery of chemotherapeutic agents to solid tumors, *Pharmacol. Rev.* 51 (1999) 691–743.
- [46] K. Xiao, Y. Li, J. Luo, J.S. Lee, W. Xiao, A.M. Gonik, R.G. Agarwal, K.S. Lam, The effect of surface charge on *in vivo* biodistribution of PEG-oligocholeic acid based micellar nanoparticles, *Biomaterials* 32 (2011) 3435–3446.
- [47] T.S. Levchenko, R. Rammohan, A.N. Lukyanov, K.R. Whiteman, V.P. Torchilin, Liposome clearance in mice: the effect of a separate and combined presence of surface charge and polymer coating, *Int. J. Pharm.* 240 (2002) 95–102.
- [48] A. Gessner, A. Lieske, B. Paulke, R. Muller, Influence of surface charge density on protein adsorption on polymeric nanoparticles: analysis by two-dimensional electrophoresis, *Eur. J. Pharm. Biopharm.* 54 (2002) 165–170.
- [49] A. Gessner, A. Lieske, B.R. Paulke, R.H. Muller, Functional groups on polystyrene model nanoparticles: influence on protein adsorption, *J. Biomed. Mater. Res. A* 65 (2003) 319–326.
- [50] J.S. Zhang, F. Liu, L. Huang, Implications of pharmacokinetic behavior of lipoplex for its inflammatory toxicity, *Adv. Drug Deliv. Rev.* 57 (2005) 689–698.
- [51] W. Li, F.C. Szoka Jr., Lipid-based nanoparticles for nucleic acid delivery, *Pharm. Res.* 24 (2007) 438–449.
- [52] M. Wang, M. Thanou, Targeting nanoparticles to cancer, *Pharmacol. Res.* 62 (2010) 90–99.
- [53] N.M. La-Beck, B.A. Zamboni, A. Gabizon, H. Schmeeda, M. Amantea, P.A. Gehrig, W.C. Zamboni, Factors affecting the pharmacokinetics of pegylated liposomal doxorubicin in patients, *Cancer Chemother. Pharmacol.* (2011).
- [54] H. Wu, R.K. Ramanathan, B.A. Zamboni, S. Strychor, S. Ramalingam, R.P. Edwards, D.M. Friedland, R.G. Stoller, C.P. Belani, L.J. Maruca, Y.J. Bang, W.C. Zamboni, Mechanism-based model characterizing bidirectional interaction between PEGylated liposomal CKD-602 (S-CKD602) and monocytes in cancer patients, *Int. J. Nanomedicine* 7 (2012) 5555–5564.
- [55] A. Gabizon, R. Isacson, O. Rosengarten, D. Tzemach, H. Shmeeda, R. Sapir, An open-label study to evaluate dose and cycle dependence of the pharmacokinetics of pegylated liposomal doxorubicin, *Cancer Chemother. Pharmacol.* 61 (2008) 695–702.
- [56] W. Lewis, The vascular pattern of tumors, *Bull. Johns Hopkins Hosp.* 41 (1927) 156–162.
- [57] J.C. Underwood, I. Carr, The ultrastructure and permeability characteristics of the blood vessels of a transplantable rat sarcoma, *J. Pathol.* 107 (1972) 157–166.
- [58] H.I. Peterson, K.L. Appelgren, Experimental studies on the uptake and retention of labeled proteins in a rat tumour, *Eur. J. Cancer* 9 (1973) 543–547.
- [59] L.E. Gerlowski, R.K. Jain, Microvascular permeability of normal and neoplastic tissues, *Microvasc. Res.* 31 (1986) 288–305.
- [60] H. Maeda, J. Takeshita, R. Kanamaru, A lipophilic derivative of neocarzinostatin. A polymer conjugation of an antitumor protein antibiotic, *Int. J. Pept. Protein Res.* 14 (1979) 81–87.
- [61] T. Konno, H. Maeda, K. Iwai, S. Maki, S. Tashiro, M. Uchida, Y. Miyauchi, Selective targeting of anti-cancer drug and simultaneous image enhancement in solid tumors by arterially administered lipid contrast medium, *Cancer* 54 (1984) 2367–2374.
- [62] H. Maeda, T. Sawa, T. Konno, Mechanism of tumor-targeted delivery of macromolecular drugs, including the EPR effect in solid tumor and clinical overview of the prototype polymeric drug SMANCS, *J. Control. Release* 74 (2001) 47–61.
- [63] H. Maeda, H. Nakamura, J. Fang, The EPR effect for macromolecular drug delivery to solid tumors: improvement of tumor uptake, lowering of systemic toxicity, and distinct tumor imaging *in vivo*, *Adv. Drug Deliv. Rev.* 65 (2013) 71–79.
- [64] K.J. Harrington, S. Mohammadtaghi, P.S. Uster, D. Glass, A.M. Peters, R.G. Vile, J.S. Stewart, Effective targeting of solid tumors in patients with locally advanced cancers by radiolabeled pegylated liposomes, *Clin. Cancer Res.* 7 (2001) 243–254.
- [65] R.K. Jain, T. Stylianopoulos, Delivering nanomedicine to solid tumors, *Nat. Rev. Clin. Oncol.* 7 (2010) 653–664.
- [66] D.W. Northfelt, B.J. Dezube, J.A. Thommes, B.J. Miller, M.A. Fischl, A. Friedman-Kien, L.D. Kaplan, C.Du. Mond, R.D. Mamelok, D.H. Henry, Pegylated-liposomal doxorubicin versus doxorubicin, bleomycin, and vincristine in the treatment of AIDS-related Kaposi's sarcoma: results of a randomized phase III clinical trial, *J. Clin. Oncol.* 16 (1998) 2445–2451.
- [67] M.E. O'Brien, N. Wiegler, M. Inbar, R. Rosso, E. Grischke, A. Santoro, R. Catane, D.G. Kieback, P. Tomczak, S.P. Ackland, F. Orlandi, L. Mellars, L. Alland, C. Tendler, Reduced cardiotoxicity and comparable efficacy in a phase III trial of pegylated liposomal doxorubicin HCl (CAELYX/Doxil) versus conventional doxorubicin for first-line treatment of metastatic breast cancer, *Ann. Oncol.* 15 (2004) 440–449.
- [68] P.S. Gill, J. Wernz, D.T. Scadden, P. Cohen, G.M. Mukwaya, J.H. von Roenn, M. Jacobs, S. Kempin, I. Silverberg, G. Gonzales, M.U. Rarick, A.M. Myers, F. Shepherd, C. Sawka, M.C. Pike, M.E. Ross, Randomized phase III trial of liposomal daunorubicin versus doxorubicin, bleomycin, and vincristine in AIDS-related Kaposi's sarcoma, *J. Clin. Oncol.* 14 (1996) 2353–2364.
- [69] A.N. Gordon, J.T. Fleagle, D. Guthrie, D.E. Parkin, M.E. Gore, A.J. Lacave, Recurrent epithelial ovarian carcinoma: a randomized phase III study of pegylated liposomal doxorubicin versus topotecan, *J. Clin. Oncol.* 19 (2001) 3312–3322.
- [70] W.J. Gradishar, S. Tjulandin, N. Davidson, H. Shaw, N. Desai, P. Bhar, M. Hawkins, J. O'Shaughnessy, Phase III trial of nanoparticle albumin-bound paclitaxel compared with polyethylated castor oil-based paclitaxel in women with breast cancer, *J. Clin. Oncol.* 23 (2005) 7794–7803.
- [71] C. Li, S. Wallace, Polymer-drug conjugates: recent development in clinical oncology, *Adv. Drug Deliv. Rev.* 60 (2008) 886–898.
- [72] R. Jain, J. Gutierrez, J. Narang, L. Scarpace, L.R. Schultz, N. Lemke, S.C. Patel, T. Mikkelsen, J.P. Rock, *In vivo* correlation of tumor blood volume and permeability with histologic and molecular angiogenic markers in gliomas, *AJNR Am. J. Neuroradiol.* 32 (2011) 388–394.
- [73] M.J. Ernsting, W.D. Foltz, E. Undzys, T. Tagami, S.D. Li, Tumor-targeted drug delivery using MR-contrasted docetaxel–carboxymethylcellulose nanoparticles, *Biomaterials* 33 (2012) 3931–3941.
- [74] T. Lammers, F. Kiessling, W.E. Hennink, G. Storm, Drug targeting to tumors: principles, pitfalls and (pre-) clinical progress, *J. Control. Release* (2011).
- [75] U. Prabhakar, H. Maeda, R.K. Jain, E.M. Sevik-Muraca, W. Zamboni, O.C. Farokhzad, S.T. Barry, A. Gabizon, P. Grodzinski, D.C. Blakey, Challenges and key considerations of the enhanced permeability and retention effect for nanomedicine drug delivery in oncology, *Cancer Res.* 73 (2013) 2412–2417.
- [76] T. Lammers, F. Kiessling, W.E. Hennink, G. Storm, Drug targeting to tumors: principles, pitfalls and (pre-) clinical progress, *J. Control. Release* 161 (2012) 175–187.
- [77] H. Cabral, Y. Matsumoto, K. Mizuno, Q. Chen, M. Murakami, M. Kimura, Y. Terada, M.R. Kano, K. Miyazono, M. Uesaka, N. Nishiyama, K. Kataoka, Accumulation of sub-100 nm polymeric micelles in poorly permeable tumours depends on size, *Nat. Nanotechnol.* 6 (2011) 815–823.

- [78] H. Lee, H. Fonge, B. Hoang, R.M. Reilly, C. Allen, The effects of particle size and molecular targeting on the intratumoral and subcellular distribution of polymeric nanoparticles, *Mol. Pharm.* 7 (2010) 1195–1208.
- [79] R.K. Jain, Determinants of tumor blood flow: a review, *Cancer Res.* 48 (1988) 2641–2658.
- [80] R.K. Jain, Normalizing tumor vasculature with anti-angiogenic therapy: a new paradigm for combination therapy, *Nat. Med.* 7 (2001) 987–989.
- [81] R.K. Jain, R.T. Tong, L.L. Munn, Effect of vascular normalization by antiangiogenic therapy on interstitial hypertension, peritumor edema, and lymphatic metastasis: insights from a mathematical model, *Cancer Res.* 67 (2007) 2729–2735.
- [82] P. Carmeliet, R.K. Jain, Angiogenesis in cancer and other diseases, *Nature* 407 (2000) 249–257.
- [83] F. Winkler, S.V. Kozin, R.T. Tong, S.S. Chae, M.F. Booth, I. Garkavtsev, L. Xu, D.J. Hicklin, D. Fukumura, E. di Tomaso, L.L. Munn, R.K. Jain, Kinetics of vascular normalization by VEGFR2 blockade governs brain tumor response to radiation: role of oxygenation, angiopoietin-1, and matrix metalloproteinases, *Cancer Cell* 6 (2004) 553–563.
- [84] R.T. Tong, Y. Boucher, S.V. Kozin, F. Winkler, D.J. Hicklin, R.K. Jain, Vascular normalization by vascular endothelial growth factor receptor 2 blockade induces a pressure gradient across the vasculature and improves drug penetration in tumors, *Cancer Res.* 64 (2004) 3731–3736.
- [85] S. Tanaka, T. Akaike, J. Wu, J. Fang, T. Sawa, M. Ogawa, T. Beppu, H. Maeda, Modulation of tumor-selective vascular blood flow and extravasation by the stable prostaglandin 12 analogue beraprost sodium, *J. Drug Target.* 11 (2003) 45–52.
- [86] C.H. Heldin, K. Rubin, K. Pietras, A. Ostman, High interstitial fluid pressure – an obstacle in cancer therapy, *Nat. Rev. Cancer* 4 (2004) 806–813.
- [87] A.L. Seynhaeve, S. Hoving, D. Schipper, C.E. Vermeulen, G. de Wiel-Ambagtsheer, S.T. van Tiel, A.M. Eggermont, T.L. Ten Hagen, Tumor necrosis factor alpha mediates homogeneous distribution of liposomes in murine melanoma that contributes to a better tumor response, *Cancer Res.* 67 (2007) 9455–9462.
- [88] T. Seki, F. Carroll, S. Illingworth, R. Cawood, V. Subr, K.D. Fisher, L.W. Seymour, Tumor necrosis factor- α increases extravasation of virus particles into tumor tissue by activating the Rho A/Rho kinase pathway, *J. Control. Release* (2013) (in press).
- [89] M.R. Kano, Y. Bae, C. Iwata, Y. Morishita, M. Yashiro, M. Oka, T. Fujii, A. Komuro, K. Kiyono, M. Kaminishi, K. Hirakawa, Y. Ouchi, N. Nishiyama, K. Kataoka, K. Miyazono, Improvement of cancer-targeting therapy, using nanocarriers for intracutable solid tumors by inhibition of TGF- β signaling, *Proc. Natl. Acad. Sci. U. S. A.* 104 (2007) 3460–3465.
- [90] L. Davies Cde, L.M. Lundstrom, J. Frengen, L. Eikenes, S.O. Bruland, O. Kaalhus, M.H. Hjelstuen, C. Brekken, Radiation improves the distribution and uptake of liposomal doxorubicin (caelyx) in human osteosarcoma xenografts, *Cancer Res.* 64 (2004) 547–553.
- [91] C. Li, S. Ke, Q.P. Wu, W. Tansey, N. Hunter, L.M. Buchmiller, L. Milas, C. Charnsangavej, S. Wallace, Tumor irradiation enhances the tumor-specific distribution of poly(L-glutamic acid)-conjugated paclitaxel and its antitumor efficacy, *Clin. Cancer Res.* 6 (2000) 2829–2834.
- [92] M.S. Anscher, L. Chen, Z. Rabbani, S. Kang, N. Larrier, H. Huang, T.V. Samulski, M.W. Dewhurst, D.M. Brizel, R.J. Folz, Z. Vujaskovic, Recent progress in defining mechanisms and potential targets for prevention of normal tissue injury after radiation therapy, *Int. J. Radiat. Oncol. Biol. Phys.* 62 (2005) 255–259.
- [93] J.H. Park, G. von Maltzahn, L. Zhang, M.P. Schwartz, E. Ruoslahti, S.N. Bhatia, M.J. Sailor, Magnetic iron oxide nanoworms for tumor targeting and imaging, *Adv. Mater.* 20 (2008) 1630–1635.
- [94] V.P. Torchilin, A.N. Lukyanov, Z. Gao, B. Papahadjopoulos-Sternberg, Immunomicelles: targeted pharmaceutical carriers for poorly soluble drugs, *Proc. Natl. Acad. Sci. U. S. A.* 100 (2003) 6039–6044.
- [95] M. Choi, K. Choi, S.W. Ryu, J. Lee, C. Choi, Dynamic fluorescence imaging for multiparametric measurement of tumor vasculature, *J. Biomed. Opt.* 16 (2011) 046008.
- [96] H. Lee, B. Hoang, H. Fonge, R.M. Reilly, C. Allen, *In vivo* distribution of polymeric nanoparticles at the whole-body, tumor, and cellular levels, *Pharm. Res.* 27 (2010) 2343–2355.
- [97] S.K. Pal, B.H. Childs, M. Pegram, Triple negative breast cancer: unmet medical needs, *Breast Cancer Res. Treat.* 125 (2011) 627–636.
- [98] R.K. Jain, Transport of molecules in the tumor interstitium: a review, *Cancer Res.* 47 (1987) 3039–3051.
- [99] J.R. Less, M.C. Posner, Y. Boucher, D. Borochovit, N. Wolmark, R.K. Jain, Interstitial hypertension in human breast and colorectal tumors, *Cancer Res.* 52 (1992) 6371–6374.
- [100] S.D. Nathanson, L. Nelson, Interstitial fluid pressure in breast cancer, benign breast conditions, and breast parenchyma, *Ann. Surg. Oncol.* 1 (1994) 333–338.
- [101] B.D. Curti, W.J. Urba, W.G. Alvord, J.E. Janik, J.W. Smith II, K. Madara, D.L. Longo, Interstitial pressure of subcutaneous nodules in melanoma and lymphoma patients: changes during treatment, *Cancer Res.* 53 (1993) 2204–2207.
- [102] B. Rippe, B. Haraldsson, Transport of macromolecules across microvascular walls: the two-pore theory, *Physiol. Rev.* 74 (1994) 163–219.
- [103] M.J. Ernsting, W.D. Foltz, E. Undzys, T. Tagami, S.D. Li, Tumor-targeted drug delivery using MR-contrasted docetaxel-carboxymethylcellulose nanoparticles, *Biomaterials* (2013) (in press).
- [104] H.F. Dvorak, Tumors: wounds that do not heal. Similarities between tumor stroma generation and wound healing, *N. Engl. J. Med.* 315 (1986) 1650–1659.
- [105] L. Ronnov-Jessen, O.W. Petersen, M.J. Bissell, Cellular changes involved in conversion of normal to malignant breast: importance of the stromal reaction, *Physiol. Rev.* 76 (1996) 69–125.
- [106] R. Kalluri, M. Zeisberg, Fibroblasts in cancer, *Nat. Rev. Cancer* 6 (2006) 392–401.
- [107] A. Aboussekhra, Role of cancer-associated fibroblasts in breast cancer development and prognosis, *Int. J. Dev. Biol.* 55 (2011) 841–849.
- [108] P.A. Netti, D.A. Berk, M.A. Swartz, A.J. Grodzinsky, R.K. Jain, Role of extracellular matrix assembly in interstitial transport in solid tumors, *Cancer Res.* 60 (2000) 2497–2503.
- [109] E.B. Brown, Y. Boucher, S. Nasser, R.K. Jain, Measurement of macromolecular diffusion coefficients in human tumors, *Microvasc. Res.* 67 (2004) 231–236.
- [110] D. Toomey, J. Harmey, C. Condron, E. Kay, D. Boucher-Hayes, Phenotyping of immune cell infiltrates in breast and colorectal tumours, *Immunol. Invest.* 28 (1999) 29–41.
- [111] H.H. van Ravenswaay Claasen, P.M. Kluijn, G.J. Fleuren, Tumor infiltrating cells in human cancer. On the possible role of CD16+ macrophages in antitumor cytotoxicity, *Lab. Invest.* 67 (1992) 166–174.
- [112] B. al-Sarireh, O. Eremin, Tumour-associated macrophages (TAMS): disordered function, immune suppression and progressive tumour growth, *J. R. Coll. Surg. Edinb.* 45 (2000) 1–16.
- [113] S.A. Shaffer, C. Baker-Lee, J. Kennedy, M.S. Lai, P. de Vries, K. Buhler, J.W. Singer, *In vitro* and *in vivo* metabolism of paclitaxel poliglumex: identification of metabolites and active proteases, *Cancer Chemother. Pharmacol.* 59 (2007) 537–548.
- [114] E.F. Jackson, E. Esparza-Coss, X. Wen, C.S. Ng, S.L. Daniel, R.E. Price, B. Rivera, C. Charnsangavej, J.G. Gelovani, C. Li, Magnetic resonance imaging of therapy-induced necrosis using gadolinium-chelated polyglutamic acids, *Int. J. Radiat. Oncol. Biol. Phys.* 68 (2007) 830–838.
- [115] D. Alizadeh, L. Zhang, J. Hwang, T. Schluep, B. Badie, Tumor-associated macrophages are predominant carriers of cyclodextrin-based nanoparticles into gliomas, *Nanomedicine* 6 (2010) 382–390.
- [116] S. Ramanujan, A. Pluen, T.D. McKee, E.B. Brown, Y. Boucher, R.K. Jain, Diffusion and convection in collagen gels: implications for transport in the tumor interstitium, *Biophys. J.* 83 (2002) 1650–1660.
- [117] N.M. La-Beck, B.A. Zamboni, A. Gabizon, H. Schmeeda, M. Amantea, P.A. Gehrig, W.C. Zamboni, Factors affecting the pharmacokinetics of pegylated liposomal doxorubicin in patients, *Cancer Chemother. Pharmacol.* 69 (2012) 43–50.
- [118] T. Stylianopoulos, M.Z. Poh, N. Insin, M.G. Bawendi, D. Fukumura, L.L. Munn, R.K. Jain, Diffusion of particles in the extracellular matrix: the effect of repulsive electrostatic interactions, *Biophys. J.* 99 (2010) 1342–1349.
- [119] O. Liele, R.M. Baumgartel, A.R. Bausch, Selective filtering of particles by the extracellular matrix: an electrostatic bandpass, *Biophys. J.* 97 (2009) 1569–1577.
- [120] T. Nomura, N. Koreeda, F. Yamashita, Y. Takakura, M. Hashida, Effect of particle size and charge on the disposition of lipid carriers after intratumoral injection into tissue-isolated tumors, *Pharm. Res.* 15 (1998) 128–132.
- [121] C.G. Willett, Y. Boucher, E. di Tomaso, D.G. Duda, L.L. Munn, R.T. Tong, D.C. Chung, D.V. Sahani, S.P. Kalva, S.V. Kozin, M. Mino, K.S. Cohen, D.T. Scadden, A.C. Hartford, A.J. Fischman, J.W. Clark, D.P. Ryan, A.X. Zhu, L.S. Blazzkowsky, H.X. Chen, P.C. Shellito, G.Y. Lauwers, R.K. Jain, Direct evidence that the VEGF-specific antibody bevacizumab has antivasculature effects in human rectal cancer, *Nat. Med.* 10 (2004) 145–147.
- [122] H.I. Hurwitz, L. Fehrenbacher, J.D. Hainsworth, W. Heim, J. Berlin, E. Holmgren, J. Hambleton, W.F. Novotny, F. Kabbinavar, Bevacizumab in combination with fluorouracil and leucovorin: an active regimen for first-line metastatic colorectal cancer, *J. Clin. Oncol.* 23 (2005) 3502–3508.
- [123] H. Wildiers, G. Guetens, G. De Boeck, E. Verbeke, B. Landuyt, W. Landuyt, E.A. de Bruijn, A.T. van Oosterom, Effect of antivasculature endothelial growth factor treatment on the intratumoral uptake of CPT-11, *Br. J. Cancer* 88 (2003) 1979–1986.
- [124] K. Pietras, Increasing tumor uptake of anticancer drugs with imatinib, *Semin. Oncol.* 31 (2004) 18–23.
- [125] K. Pietras, A. Ostman, M. Sjoquist, E. Buchdunger, R.K. Reed, C.H. Heldin, K. Rubin, Inhibition of platelet-derived growth factor receptors reduces interstitial hypertension and increases transcapillary transport in tumors, *Cancer Res.* 61 (2001) 2929–2934.
- [126] R. Cairns, I. Papandreou, N. Denko, Overcoming physiologic barriers to cancer treatment by molecularly targeting the tumor microenvironment, *Mol. Cancer Res.* 4 (2006) 61–70.
- [127] M. Murakami, M.J. Ernsting, E. Undzys, N. Holwell, W.D. Foltz, S.D. Li, Docetaxel conjugate nanoparticles that target α -smooth muscle actin-expressing stromal cells suppress breast cancer metastasis, *Cancer Res.* (2013) (in press).
- [128] T.P. Padera, B.R. Stoll, J.B. Tooredman, D. Capen, E. di Tomaso, R.K. Jain, Pathology: cancer cells compress intratumour vessels, *Nature* 427 (2004) 695.
- [129] D.C. Von Hoff, R.K. Ramanathan, M.J. Borad, D.A. Laheru, L.S. Smith, T.E. Wood, R.L. Korn, N. Desai, V. Trieu, J.L. Iglesias, H. Zhang, P. Soon-Shiong, T. Shi, N.V. Rajeshkumar, A. Maitra, M. Hidalgo, Gemcitabine plus nab-paclitaxel is an active regimen in patients with advanced pancreatic cancer: a phase I/II trial, *J. Clin. Oncol.* 29 (2011) 4548–4554.
- [130] K.P. Olive, M.A. Jacobetz, C.J. Davidson, A. Gopinathan, D. McIntyre, D. Honess, B. Madhu, M.A. Goldgraben, M.E. Caldwell, D. Allard, K.K. Frese, G. Denicola, C. Feig, C. Combs, S.P. Winter, H. Ireland-Zecchini, S. Reichelt, W.J. Howat, A. Chang, M. Dhara, L. Wang, F. Ruckert, R. Grutzmann, C. Pilarsky, K. Izeradjene, S.R. Hingorani, P. Huang, S.E. Davies, W. Plunkett, M. Egorin, R.H. Hruban, N. Whitebread, K. McGovern, J. Adams, C. Iacobuzio-Donahue, J. Griffiths, D.A. Tuveson, Inhibition of Hedgehog signaling enhances delivery of chemotherapy in a mouse model of pancreatic cancer, *Science* 324 (2009) 1457–1461.
- [131] D. Hanahan, R.A. Weinberg, Hallmarks of cancer: the next generation, *Cell* 144 (2011) 646–674.
- [132] T.L. Andresen, S.S. Jensen, K. Jorgensen, Advanced strategies in liposomal cancer therapy: problems and prospects of active and tumor specific drug release, *Prog. Lipid Res.* 44 (2005) 68–97.
- [133] K.M. Laginha, S. Verwoert, G.J. Charrois, T.M. Allen, Determination of doxorubicin levels in whole tumor and tumor nuclei in murine breast cancer tumors, *Clin. Cancer Res.* 11 (2005) 6944–6949.

- 1342 [134] A. Gabizon, H. Shmeeda, Y. Barenholz, Pharmacokinetics of pegylated liposomal
1343 Doxorubicin: review of animal and human studies, *Clin. Pharmacokinet.* 42
1344 (2003) 419–436.
- 1345 [135] K.J. Harrington, C.R. Lewanski, A.D. Northcote, J. Whittaker, H. Wellbank, R.G. Vile,
1346 A.M. Peters, J.S. Stewart, Phase I–II study of pegylated liposomal cisplatin (SPI-077)
1347 in patients with inoperable head and neck cancer, *Ann. Oncol.* 12 (2001) 493–496.
- 1348 [136] W.T. Lim, E.H. Tan, C.K. Toh, S.W. Hee, S.S. Leong, P.C. Ang, N.S. Wong, B. Chowbay,
1349 Phase I pharmacokinetic study of a weekly liposomal paclitaxel formulation
1350 (Genexol-PM) in patients with solid tumors, *Ann. Oncol.* 21 (2010) 382–388.
- 1351 [137] T. Hamaguchi, Y. Matsumura, M. Suzuki, K. Shimizu, R. Goda, I. Nakamura, I. Nakatomi,
1352 M. Yokoyama, K. Kataoka, T. Kakizoe, NK105, a paclitaxel-incorporating micellar
1353 nanoparticle formulation, can extend *in vivo* antitumor activity and reduce the neuro-
1354 rotoxicity of paclitaxel, *Br. J. Cancer* 92 (2005) 1240–1246.
- 1355 [138] G. Gaucher, R.H. Marchessault, J.C. Leroux, Polyester-based micelles and nanoparticles
1356 for the parenteral delivery of taxanes, *J. Control. Release* 143 (2010) 2–12.
- 1357 [139] K. Letchford, R. Liggins, K.M. Wasan, H. Burt, *In vitro* human plasma distribution of
1358 nanoparticulate paclitaxel is dependent on the physicochemical properties of
1359 poly(ethylene glycol)-block-poly(caprolactone) nanoparticles, *Eur. J. Pharm.*
1360 *Biopharm.* 71 (2009) 196–206.
- 1361 [140] E. Miele, G.P. Spinelli, F. Tomao, S. Tomao, Albumin-bound formulation of paclitaxel
1362 (Abraxane ABI-007) in the treatment of breast cancer, *Int. J. Nanomedicine* 4
1363 (2009) 99–105.
- 1364 [141] M. Harries, P. Ellis, P. Harper, Nanoparticle albumin-bound paclitaxel for metastatic
1365 breast cancer, *J. Clin. Oncol.* 23 (2005) 7768–7771.
- 1366 [142] D.W. Nyman, K.J. Campbell, E. Hersh, K. Long, K. Richardson, V. Trieu, N. Desai, M.J.
1367 Hawkins, D.D. Von Hoff, Phase I and pharmacokinetics trial of ABI-007, a novel
1368 nanoparticle formulation of paclitaxel in patients with advanced nonhematologic
1369 malignancies, *J. Clin. Oncol.* 23 (2005) 7785–7793.
- 1370 [143] A.V. Boddy, E.R. Plummer, R. Todd, J. Sludden, M. Griffin, L. Robson, J. Cassidy, D.
1371 Bissett, A. Bernareggi, M.W. Verrill, A.H. Calvert, A phase I and pharmacokinetic
1372 study of paclitaxel poliglumex (XYOTAX), investigating both 3-weekly and
1373 2-weekly schedules, *Clin. Cancer Res.* 11 (2005) 7834–7840.
- 1374 [144] C. Li, R.A. Newman, Q.P. Wu, S. Ke, W. Chen, T. Hutto, Z. Kan, M.D. Brannan, C.
1375 Charnsangavej, S. Wallace, Biodistribution of paclitaxel and poly(L-glutamic
1376 acid)-paclitaxel conjugate in mice with ovarian OCa-1 tumor, *Cancer*
1377 *Chemother. Pharmacol.* 46 (2000) 416–422.
- 1378 [145] S.D. Conner, S.L. Schmid, Regulated portals of entry into the cell, *Nature* 422 (2003)
1379 37–44.
- 1380 [146] F. Zhao, Y. Zhao, Y. Liu, X. Chang, C. Chen, Y. Zhao, Cellular uptake, intracellular traf-
1381 ficking, and cytotoxicity of nanomaterials, *Small* 7 (2011) 1322–1337.
- 1382 [147] J. Wang, J.D. Byrne, M.E. Napier, J.M. DeSimone, More effective nanomedicines
1383 through particle design, *Small* 7 (2011) 1919–1931.
- 1384 [148] T.M. Allen, P.R. Cullis, Liposomal drug delivery systems: from concept to clinical ap-
1385 plications, *Adv. Drug Deliv. Rev.* 65 (2013) 36–48.
- 1386 [149] A. Koshkaryev, R. Sawant, M. Deshpande, V. Torchilin, Immunoconjugates and long
1387 circulating systems: origins, current state of the art and future directions, *Adv.*
1388 *Drug Deliv. Rev.* 65 (2013) 24–35.
- 1389 [150] A.S. Hoffman, Stimuli-responsive polymers: biomedical applications and chal-
1390 lenges for clinical translation, *Adv. Drug Deliv. Rev.* 65 (2013) 10–16.
- 1391 [151] W. Arap, W. Haedicke, M. Bernasconi, R. Kain, D. Rajotte, S. Krajewski, H.M. Ellerby,
1392 D.E. Bredesen, R. Pasqualini, E. Ruoslahti, Targeting the prostate for destruction
1393 through a vascular address, *Proc. Natl. Acad. Sci. U. S. A.* 99 (2002) 1527–1531.
- 1394 [152] S.E. Gratton, P.A. Ropp, P.D. Pohlhaus, J.C. Luft, V.J. Madden, M.E. Napier, J.M.
1395 DeSimone, The effect of particle design on cellular internalization pathways,
1396 *Proc. Natl. Acad. Sci. U. S. A.* 105 (2008) 11613–11618.
- 1397 [153] W. Jiang, B.Y. Kim, J.T. Rutka, W.C. Chan, Nanoparticle-mediated cellular response is
1398 size-dependent, *Nat. Nanotechnol.* 3 (2008) 145–150.
- 1399 [154] X. Huang, X. Teng, D. Chen, F. Tang, J. He, The effect of the shape of mesoporous sil-
1400 ica nanoparticles on cellular uptake and cell function, *Biomaterials* 31 (2010)
1401 438–448.
- 1402 [155] B.D. Chithrani, A.A. Ghazani, W.C. Chan, Determining the size and shape depen-
1403 dence of gold nanoparticle uptake into mammalian cells, *Nano Lett.* 6 (2006)
1404 662–668.
- 1405 [156] K. Zhang, H. Fang, Z. Chen, J.S. Taylor, K.L. Wooley, Shape effects of nanoparticles
1406 conjugated with cell-penetrating peptides (HIV Tat PTD) on CHO cell uptake,
1407 *Bioconjug. Chem.* 19 (2008) 1880–1887.
- 1408 [157] X. Guo, F.C. Szoka Jr., Steric stabilization of fusogenic liposomes by a low-pH sensi-
1409 tive PEG–diortho ester–lipid conjugate, *Bioconjug. Chem.* 12 (2001) 291–300.
- 1410 [158] A.A. Kale, V.P. Torchilin, Enhanced transfection of tumor cells *in vivo* using “Smart”
1411 pH-sensitive TAT-modified pegylated liposomes, *J. Drug Target.* 15 (2007)
1412 538–545.
- 1413 [159] L. Zhu, P. Kate, V.P. Torchilin, Matrix metalloproteinase 2-responsive multifunctional li-
1414 posomal nanocarrier for enhanced tumor targeting, *ACS Nano* 6 (2012) 3491–3498.
- 1415 [160] S.C. Semple, A. Akinc, J. Chen, A.P. Sandhu, B.L. Mui, C.K. Cho, D.W. Sah, D. Stebbing,
1416 E.J. Crossley, E. Yaworski, I.M. Hafez, J.R. Dorkin, J. Qin, K. Lam, K.G. Rajeev, K.F.
1417 Wong, L.B. Jeffs, L. Nechev, M.L. Eisenhardt, M. Jayaraman, M. Kazem, M.A. Maier,
1418 M. Srinivasulu, M.J. Weinstein, Q. Chen, R. Alvarez, S.A. Barros, S. De, S.K. Klimuk,
1419 T. Borland, V. Kosovrasti, W.L. Cantley, Y.K. Tam, M. Manoharan, M.A. Ciufolini,
1420 M.A. Tracy, A. de Fougerolles, I. MacLachlan, P.R. Cullis, T.D. Madden, M.J. Hope, Ra-
1421 tional design of cationic lipids for siRNA delivery, *Nat. Biotechnol.* 28 (2010)
1422 172–176.
- 1423 [161] T. Osaka, T. Nakanishi, S. Shanmugam, S. Takahama, H. Zhang, Effect of surface
1424 charge of magnetite nanoparticles on their internalization into breast cancer and
1425 umbilical vein endothelial cells, *Colloids Surf. B Biointerfaces* 71 (2009) 325–330.
- 1426 [162] A. Santel, M. Aleku, O. Keil, J. Endruschat, V. Esche, G. Fisch, S. Dames, K. Löffler, M.
1427 Fechtner, W. Arnold, K. Giese, A. Klippel, J. Kaufmann, A novel siRNA–lipoplex tech-
1428 nology for RNA interference in the mouse vascular endothelium, *Gene Ther.* 13
1429 (2006) 1222–1234.
- 1430 [163] T.H. Chung, S.H. Wu, M. Yao, C.W. Lu, Y.S. Lin, Y. Hung, C.Y. Mou, Y.C. Chen, D.M.
1431 Huang, The effect of surface charge on the uptake and biological function of
1432 mesoporous silica nanoparticles in 3T3-L1 cells and human mesenchymal stem
1433 cells, *Biomaterials* 28 (2007) 2959–2966.
- 1434 [164] S.D. Li, L. Huang, Nanoparticles evading the reticuloendothelial system: role of the
1435 supported bilayer, *Biochim. Biophys. Acta* 1788 (2009) 2259–2266.
- 1436 [165] I. MacLachlan, P. Cullis, Diffusible-PEG–lipid stabilized plasmid lipid particles, *Adv.*
1437 *Genet.* 53PA (2005) 157–188.
- 1438 [166] J.S. Choi, J.A. MacKay, F.C. Szoka Jr., Low-pH-sensitive PEG-stabilized plasmid–lipid
1439 nanoparticles: preparation and characterization, *Bioconjug. Chem.* 14 (2003)
1440 420–429.
- 1441 [167] D.B. Kirpotin, D.C. Drummond, Y. Shao, M.R. Shalaby, K. Hong, U.B. Nielsen, J.D. Marks,
1442 C.C. Benz, J.W. Park, Antibody targeting of long-circulating lipidic nanoparticles does
1443 not increase tumor localization but does increase internalization in animal models,
1444 *Cancer Res.* 66 (2006) 6732–6740.
- 1445 [168] K. McNeeley, A. Annapragada, R. Bellamkonda, Decreased circulation time offsets
1446 increased efficacy of PEGylated nanocarriers targeting folate receptors of glioma,
1447 *Nanotechnology* 18 (2007) 385101.
- 1448 [169] W.C. Chen, G.C. Completo, D.S. Sigal, P.R. Crocker, A. Saven, J.C. Paulson, *In vivo*
1449 targeting of B-cell lymphoma with glycan ligands of CD22, *Blood* 115 (2010)
1450 4778–4786.
- 1451 [170] S. Muro, New biotechnological and nanomedicine strategies for treatment of lysoso-
1452 mal storage disorders, *Wiley Interdiscip. Rev. Nanomed. Nanobiotechnol.* 2
1453 (2010) 189–204.
- 1454 [171] D.W. Bartlett, H. Su, I.J. Hildebrandt, W.A. Weber, M.E. Davis, Impact of tumor-
1455 specific targeting on the biodistribution and efficacy of siRNA nanoparticles
1456 measured by multimodality *in vivo* imaging, *Proc. Natl. Acad. Sci. U. S. A.* 104
1457 (2007) 15549–15554.
- 1458 [172] S.H. Pun, F. Tack, N.C. Bellocq, J. Cheng, B.H. Grubbs, G.S. Jensen, M.E. Davis, M.
1459 Brewster, M. Janicot, B. Janssens, W. Floren, A. Bakker, Targeted delivery of
1460 RNA-cleaving DNA enzyme (DNAzyme) to tumor tissue by transferrin-modified,
1461 cyclodextrin-based particles, *Cancer Biol. Ther.* 3 (2004) 641–650.
- 1462 [173] S.D. Li, Y.C. Chen, M.J. Hackett, L. Huang, Tumor-targeted delivery of siRNA by
1463 self-assembled nanoparticles, *Mol. Ther.* 16 (2008) 163–169.
- 1464 [174] W.C. Zamboni, J.L. Eiseman, S. Strychor, P.M. Rice, E. Joseph, B.A. Zamboni, M.K.
1465 Donnelly, J. Shurer, R.A. Parise, M.E. Tonda, N.Y. Yu, P.H. Basse, Tumor disposition
1466 of pegylated liposomal CKD-602 and the reticuloendothelial system in preclinical
1467 tumor models, *J. Liposome Res.* 21 (2011) 70–80.
- 1468 [175] S.D. Li, L. Huang, Stealth nanoparticles: high density but sheddable PEG is a key for
1469 tumor targeting, *J. Control. Release* 145 (2010) 178–181.
- 1470 [176] Y. Yang, J. Li, F. Liu, L. Huang, Systemic delivery of siRNA via LCP nanoparticle effi-
1471 ciently inhibits lung metastasis, *Mol. Ther.* 20 (2012) 609–615.
- 1472 [177] W.P. Caron, G. Song, P. Kumar, S. Rawal, W.C. Zamboni, Interpatient pharmacoki-
1473 netic and pharmacodynamic variability of carrier-mediated anticancer agents,
1474 *Clin. Pharmacol. Ther.* 91 (2012) 802–812.
- 1475 [178] E. Karathanasis, S. Suryanarayanan, S.R. Balusu, K. McNeeley, I. Sechopoulos, A.
1476 Karellas, A.V. Annapragada, R.V. Bellamkonda, Imaging nanoprobe for prediction
1477 of outcome of nanoparticle chemotherapy by using mammography, *Radiology*
1478 250 (2009) 398–406.
- 1479 [179] T. Tagami, M.J. Ernsting, S.D. Li, Efficient tumor regression by a single and low dose
1480 treatment with a novel and enhanced formulation of thermosensitive liposomal
1481 doxorubicin, *J. Control. Release* 152 (2011) 303–309.
- 1482 [180] T. Tagami, M.J. Ernsting, S.D. Li, Optimization of a novel and improved
1483 thermosensitive liposome formulated with DPPE and a Brij surfactant using a ro-
1484 bust *in vitro* system, *J. Control. Release* 154 (2011) 290–297.
- 1485 [181] T. Tagami, W.D. Foltz, M.J. Ernsting, C.M. Lee, I.F. Tannock, J.P. May, S.D. Li, MRI mon-
1486 itoring of intratumoral drug delivery and prediction of the therapeutic effect with a
1487 multifunctional thermosensitive liposome, *Biomaterials* 32 (2011) 6570–6578.
- 1488 [182] T. Tagami, J.P. May, M.J. Ernsting, S.D. Li, A thermosensitive liposome prepared with
1489 a Cu₂+ gradient demonstrates improved pharmacokinetics, drug delivery and
1490 antitumor efficacy, *J. Control. Release* (2012).
- 1491 [183] D. Needham, M.W. Dewhirst, The development and testing of a new
1492 temperature-sensitive drug delivery system for the treatment of solid tu-
1493 mors, *Adv. Drug Deliv. Rev.* 53 (2001) 285–305.
- 1494 [184] A.B. Simonson, J.E. Schnitzer, Vascular proteomic mapping *in vivo*, *J. Thromb.*
1495 *Haemost.* 5 (Suppl. 1) (2007) 183–187.